



GOBIERNO DE ESPAÑA

MINISTERIO DE CIENCIA E INNOVACIÓN



AGENCIA ESTATAL DE INVESTIGACIÓN



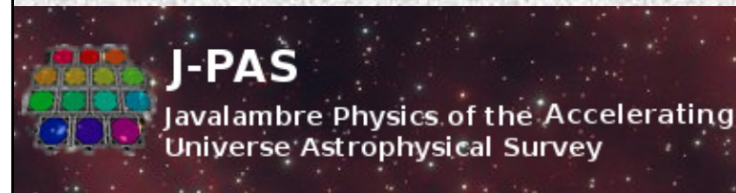
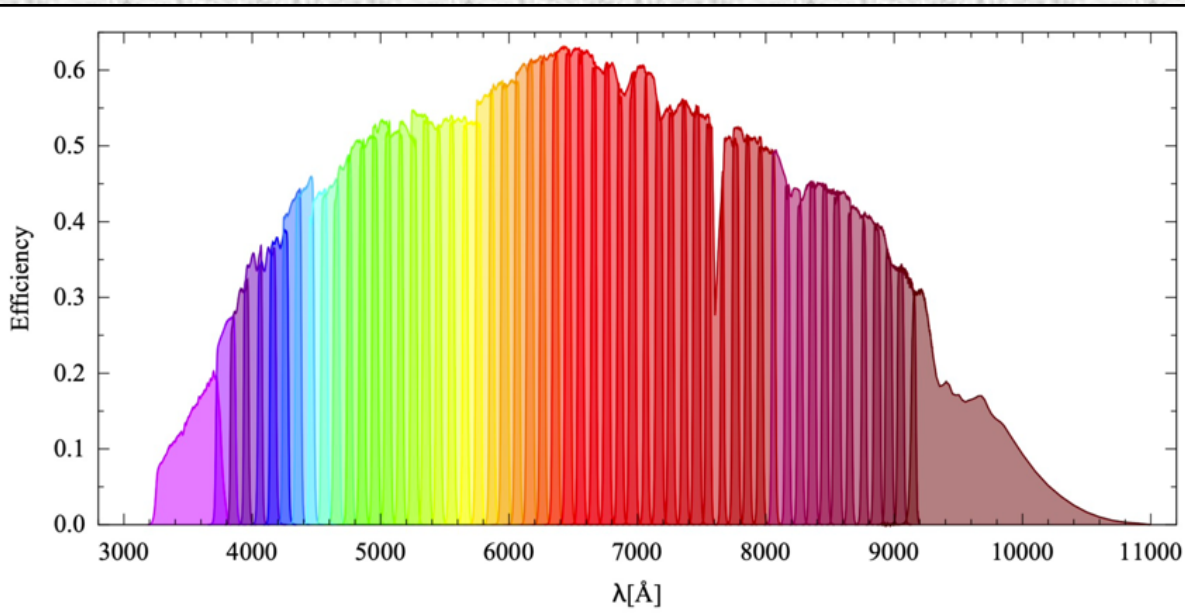
Universidad de La Laguna



EXCELENCIA SEVERO OCHOA

PID2021-126616NB-I00

Indiscriminate $R \sim 50$ spectroscopy in the entire footprint: the spectro-photometric approach of J-PAS



Carlos Hernández-Monteagudo (IAC/ULL)

On behalf of the J-PAS collaboration

Outline

- Spectro-photometry as midway approach to full spectroscopic and photometric surveys
- The Javalambre PAU Astrophysical Survey (J-PAS)
- Predictions versus first observations in miniJPAS and J-NEP: depth, photo-z precision and accuracy, and galaxy cluster and group abundances
- Prospects for Dark Energy Probes: Multi-probe clustering, galaxy clusters, and QSOs
- Current status and forecasts for the future

Photometry

vs.

Spectroscopy

- Unbiased samples
- Faster & cheaper
- Large Volumes
- High number density

- SED of targets
- Precise redshifts

Photometry

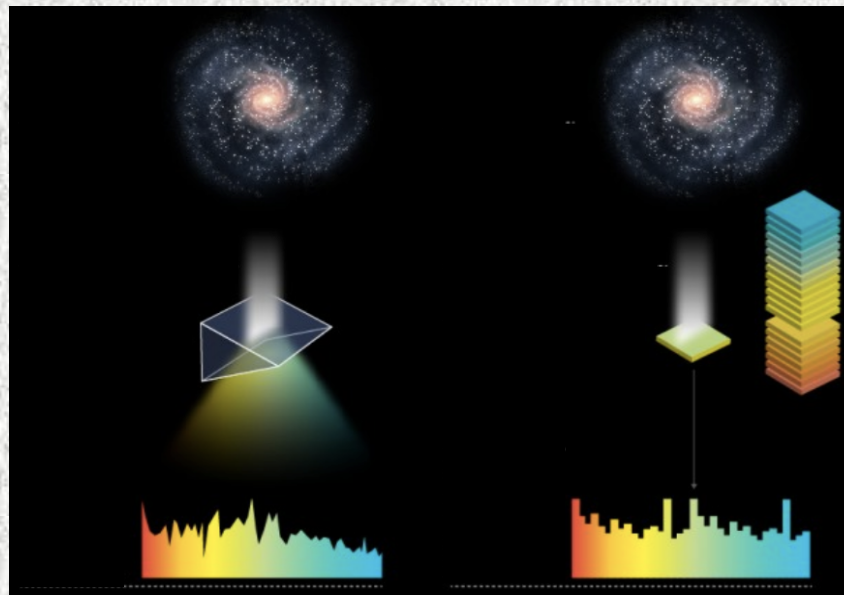
- Unbiased samples
- Faster & cheaper
- Large Volumes
- High number density

vs.

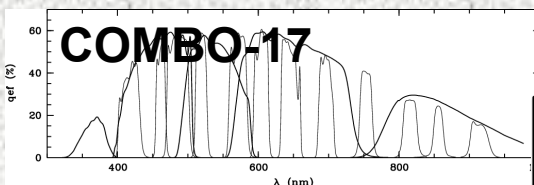
Spectroscopy

- SED of targets
- Precise redshifts

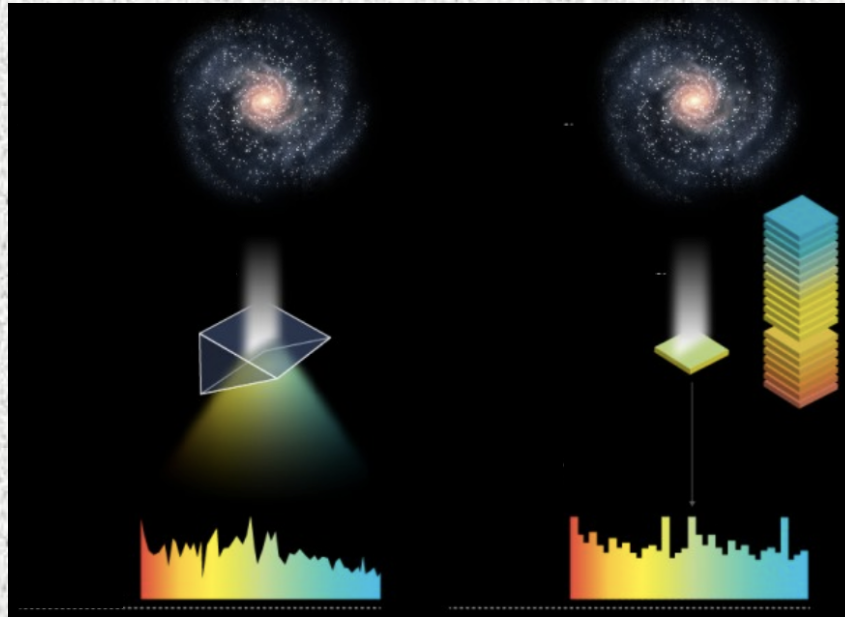
Spectro-Photometry



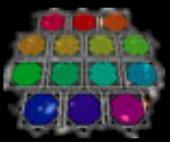
This provides a *low resolution* ($R \sim 50$) pseudo-spectrum in *every pixel* of the footprint



Spectro-Photometry



Javalambre Photometric Local
Universe Survey



J-PAS

Javalambre Physics of the Accelerating
Universe Astrophysical Survey



The *Observatorio Astrofísico de Javalambre (OAJ)*



*Pico del Buitre (Vulture's Peak),
By Arcos de las Salinas, about
60' from Teruel and 80' from
Valencia*



The Observatorio Astrofísico de Javalambre (OAJ)



*Pico del Buitre (Vulture's Peak),
By Arcos de las Salinas, about
60' from Teruel and 80' from
Valencia*

EL PAÍS

ANDALUCÍA CATALUÑA C. VALENCIANA GALICIA MADRID PAÍS VASCO MÁS COMUNID

La Laponia española

La región de los Montes Universales, entre Teruel y Cuenca, tiene una densidad de población similar a la de Laponia. Un recorrido por esta zona permite ver cómo es la aislada vida de esta región.

NACHO CARRETERO

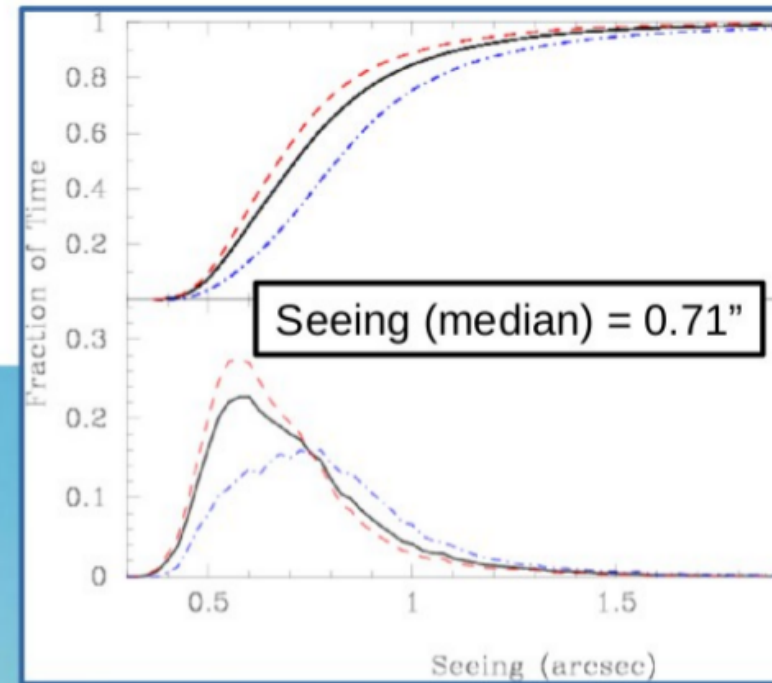
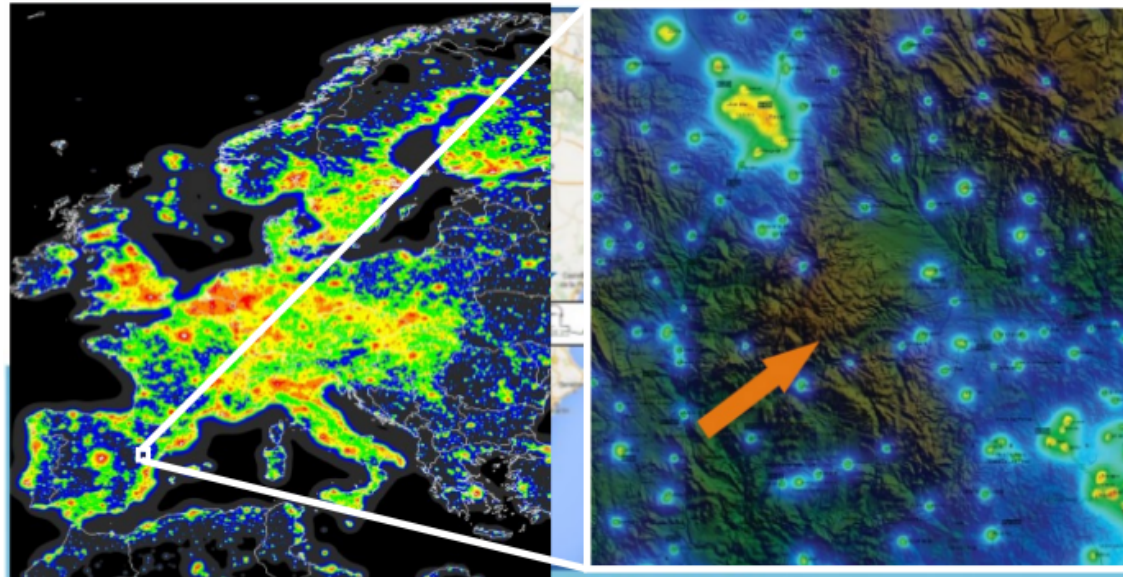
The "Spanish Lapland"

En los Montes Universales, un territorio del tamaño de Guipúzcoa, la densidad de población es de 1,63 habitantes por km². En Laponia, la región más septentrional de Escandinavia, hay 1,87.



The Javalambre Observatory (OAJ)

In the “Sierra de Javalambre” @1960m
now officially a Spanish “scientific and technical facility” (20% available for open-time)



JST (T250)

JAST (T80)



The OAJ exploits the niche of a site and instrumentation devoted to **spectro-photometric** surveys: telescopes with **wide field-of-views** and **multi-narrow band filter** systems

The Telescopes



M1 (\emptyset) = 2.55 m
FoV (\emptyset) = 3 deg = 476 mm
at FP
Etendue = 27.5 m²deg²

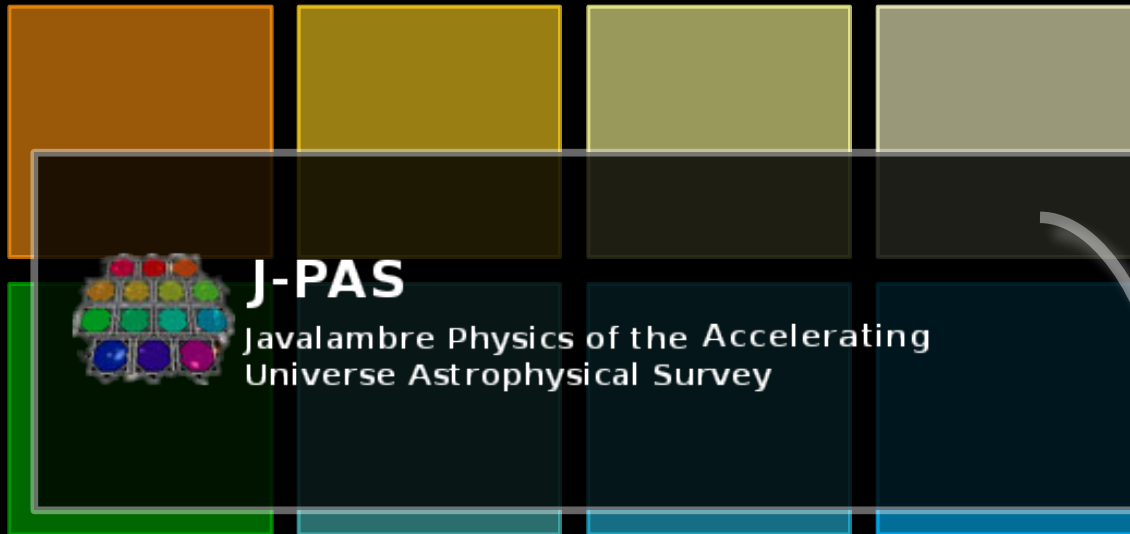
Currently
equipped with
the “pathfinder”
camera

M1 (\emptyset) = 0.8 m
FoV (\emptyset) = 2 deg



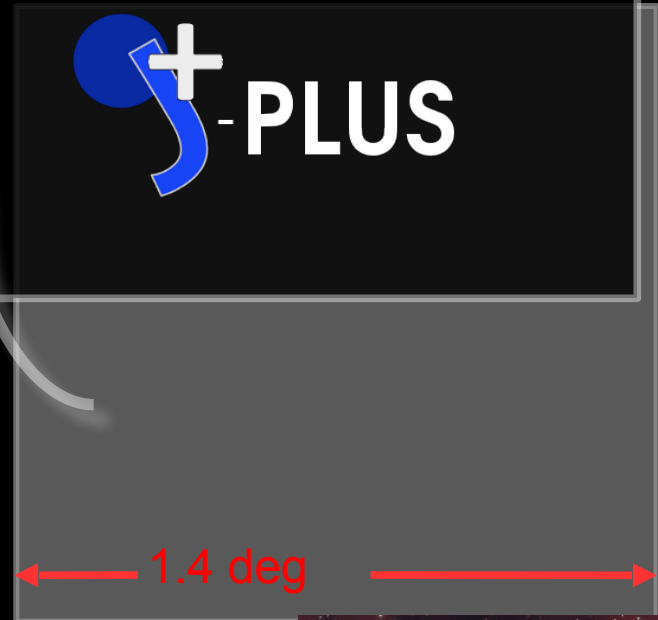
JPCam

T80Cam



J-PAS

Javalambre Physics of the Accelerating
Universe Astrophysical Survey

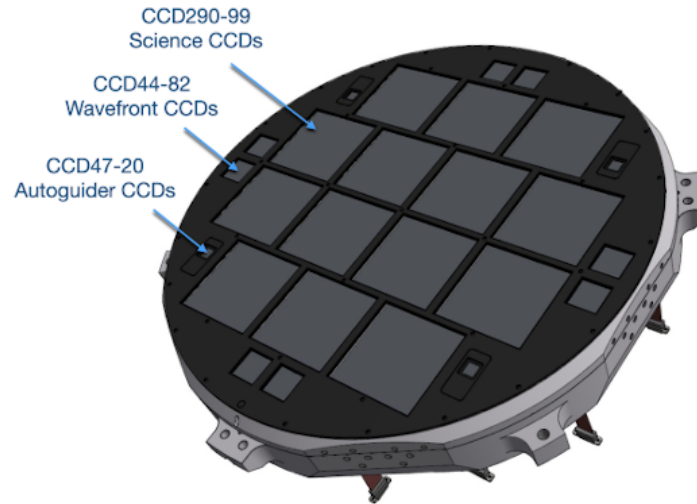


J-PLUS

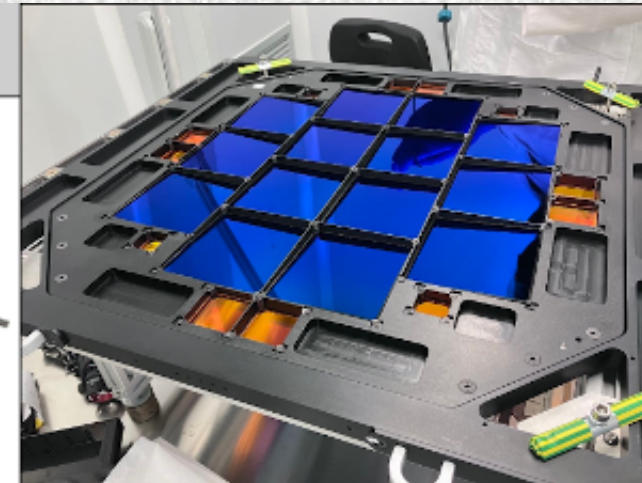
1.4 deg

The camera JPCam

1.2 Giga pixels
(14 CCD of
9200x9200)
0.22 arcsec/pixel
4.5 deg²

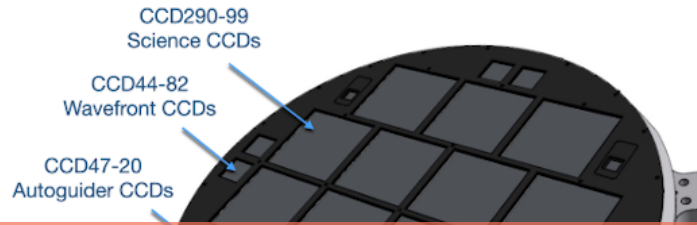


Filter trays (x5 + x3)



The camera

JPCam



	Telescope		Camera				
	Size	FoV	# CCDs	CCD format	# of pixels	Resolution	Filters
LSST	8.4m	9.6 sq. deg.	189	4096 x 4096	3.2 Gpixels	0.2"/pix	u, g, r, i, z, y
PanStarrs	1.8m	6.7 sq. deg.	60	4600 x 4600	1.3 Gpixels	0.26"/pix	g, r, i, z, y
JPCam	2.5m	4.9 sq. deg.	14	9231 x 9216	1.2 Gpixels	0.23"/pix	54NB + 2BB
HyperSuprimeCam	8.2m	1.8 sq. deg.	112	2048 x 4096	940 Mpixels	0.18"/pix	r, i, z, y
VIS (Euclid)	1.2m	0.5 sq. deg.	36	4096 x 4096	520 Mpixels	0.1"/pix	R, I, Z
DECam	4m	3 sq. deg.	62	2048 x 4096	500 Mpixels	0.27"/pix	g, r, i, z, y
Megacam	3.6m	1 sq. deg.	32	2048 x 4096	340 Mpixels	0.19"/pix	u, g, r, i, z
Omegacam	2.6m	1 sq. deg.	32	2048 x 4096	340 Mpixels	0.21"/pix	u, g, r, i, z
JPAS-Path Finder	2.5m	0.45 sq. deg.	1	10580x10560	110 Mpixels	0.23"/pix	g, r, i + NBs
T80Cam	0.8m	2.1 sq. deg.	1	10580x10560	110 Mpixels	0.5"/pix	u, g, r, i, z + 7NB
SuprimeCam	8.2m	0.25 sq. deg.	10	2048 x 4096	80 Mpixels	0.2"/pix	g, r, i, z, y

J-PAS filter system

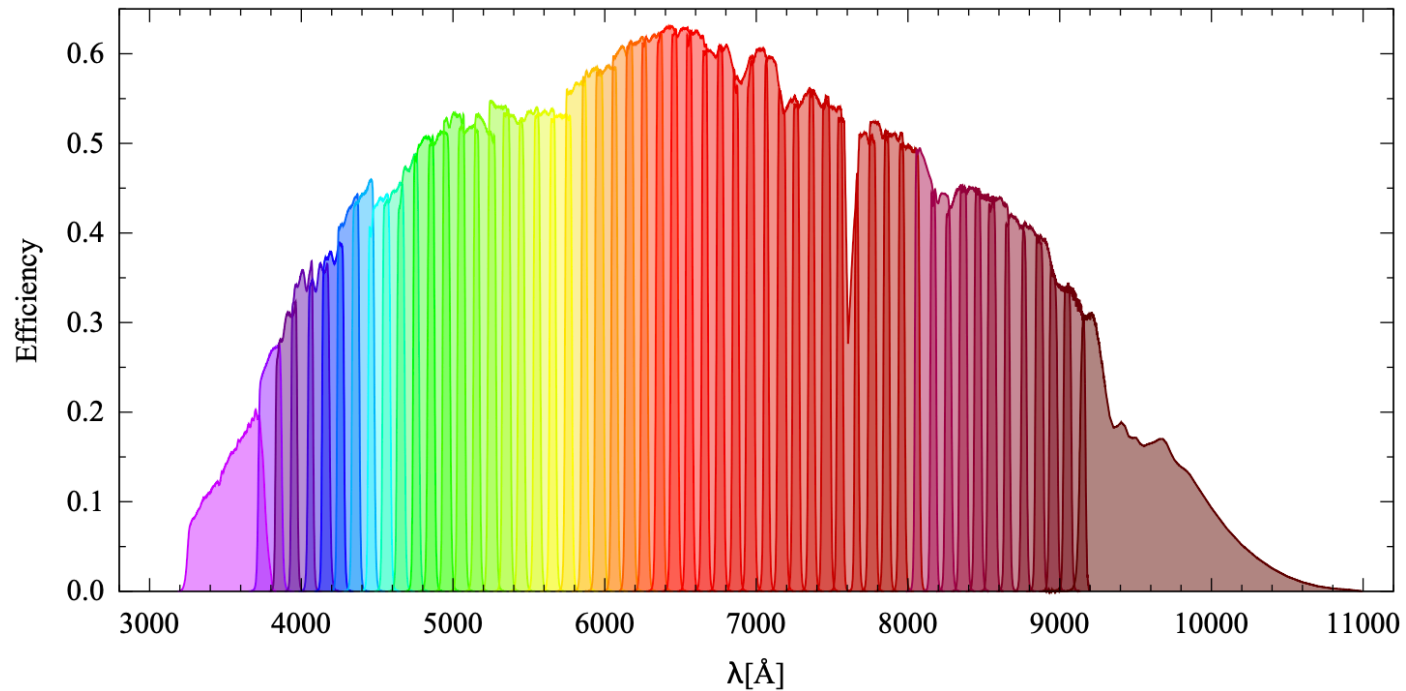


Fig. 2: The measured transmission curves of the J-PAS filters. Effects of the CCD quantum efficiency, the entire optical system of the JST/T250 telescope and sky absorption are included. The HTML color representation of each filter is provided in the miniJPAS database in the table `minijpas.Filter`.

Table 3: Filter system main characteristics. The full table is available in the miniJPAS database in the ADQL table `minijpas.Filter`.

Filter #	Filter name	Central Wavelength [Å]	FWHM [Å]
1	<i>uJAVA</i>	3497	495
2	<i>J0378</i>	3782	155
3	<i>J0390</i>	3904	145
4	<i>J0400</i>	3996	145
5	<i>J0410</i>	4110	145
...
54	<i>J0900</i>	9000	145
55	<i>J0910</i>	9107	145
56	<i>J1007</i>	9316	<i>High-pass filter</i>

The filter system

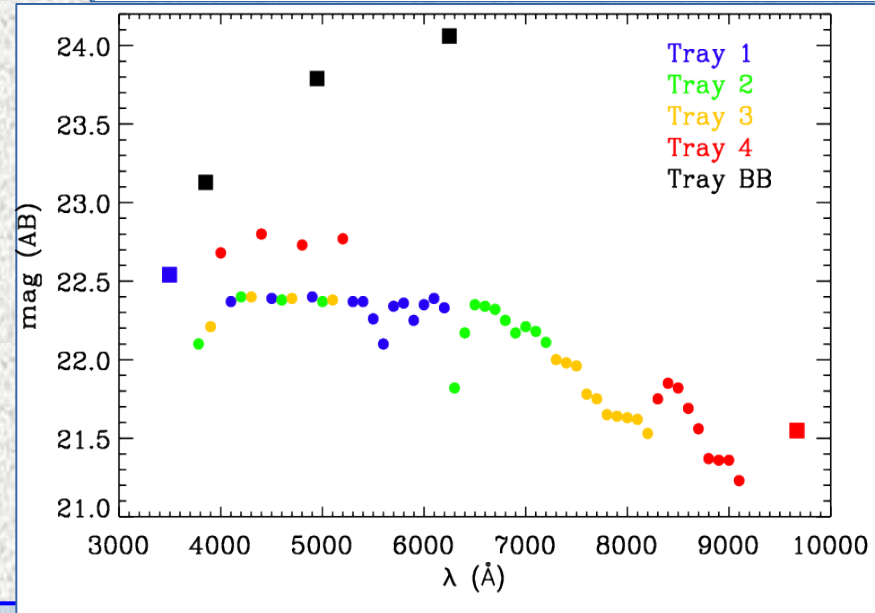
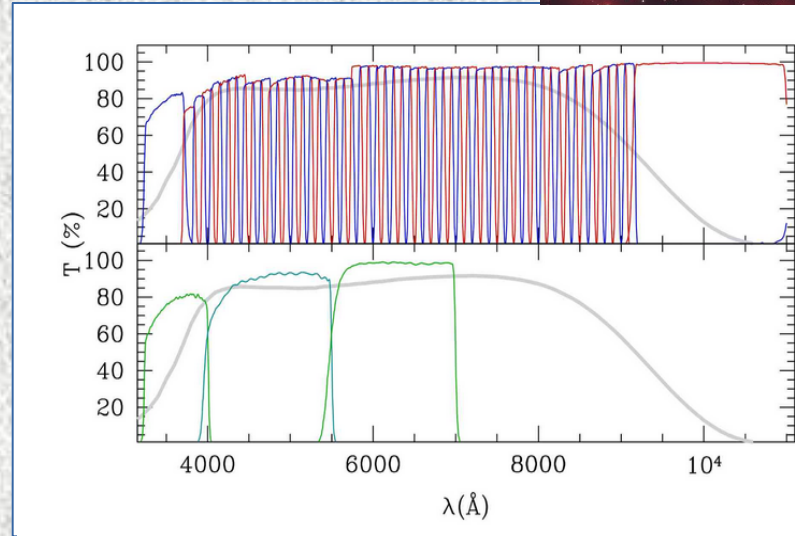


- **54 NB filters**
(FWHM~145Å;
 $\Delta\lambda\sim 10\text{nm}$)
From 3785Å to
9100Å

- **1 Blue MB filter**
(FWHM~260Å;
 $\lambda_c\sim 3600\text{Å}$)

- **1 Red BB filter**
(FWHM~620Å;
 $\lambda_c\sim 9500\text{Å}$)

- **Sloan *i*-band**



5σ
3" aperture

Pseudo-spectrum (R~50) for every pixel of the sky

The filter system

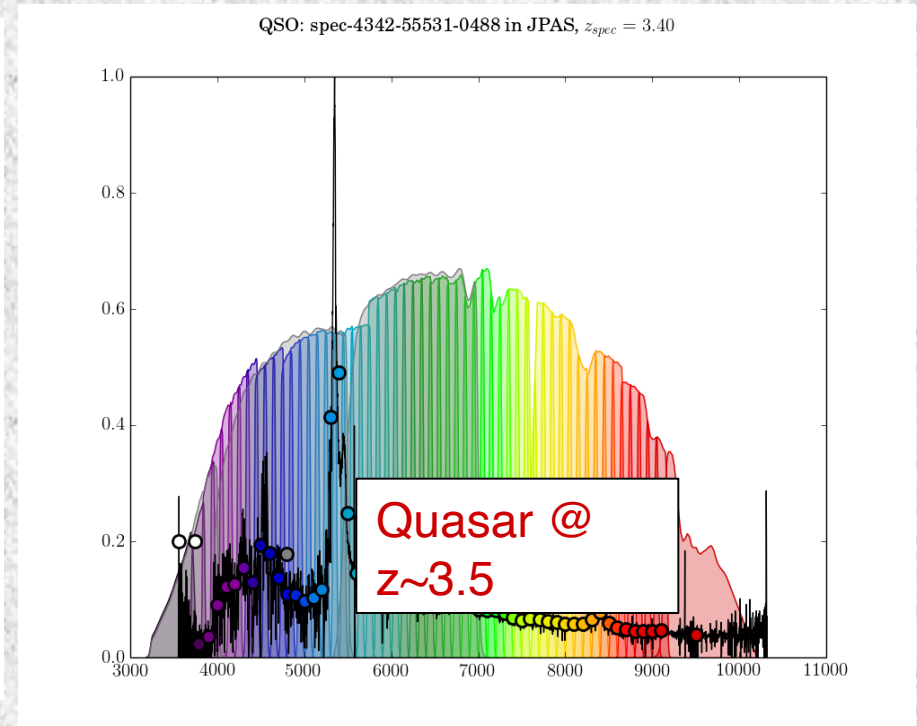
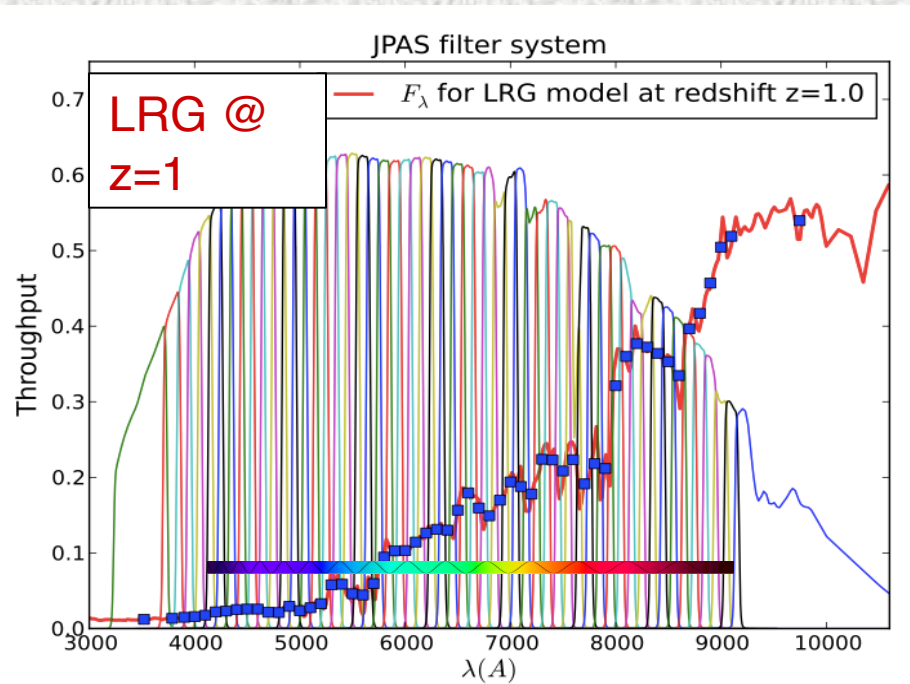
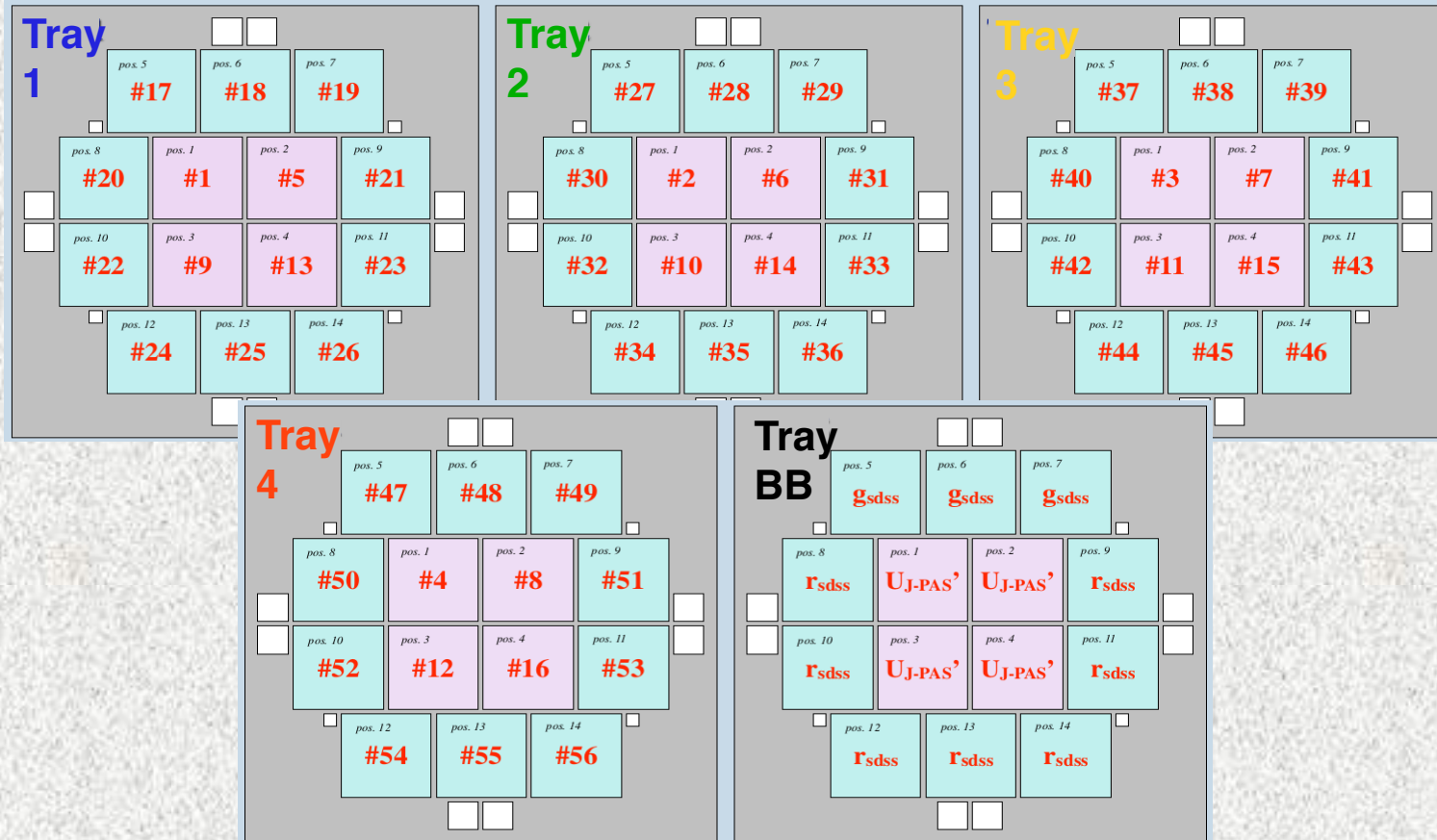


Photo-z precision as
good as $0.003(1+z)$

The camera + filters

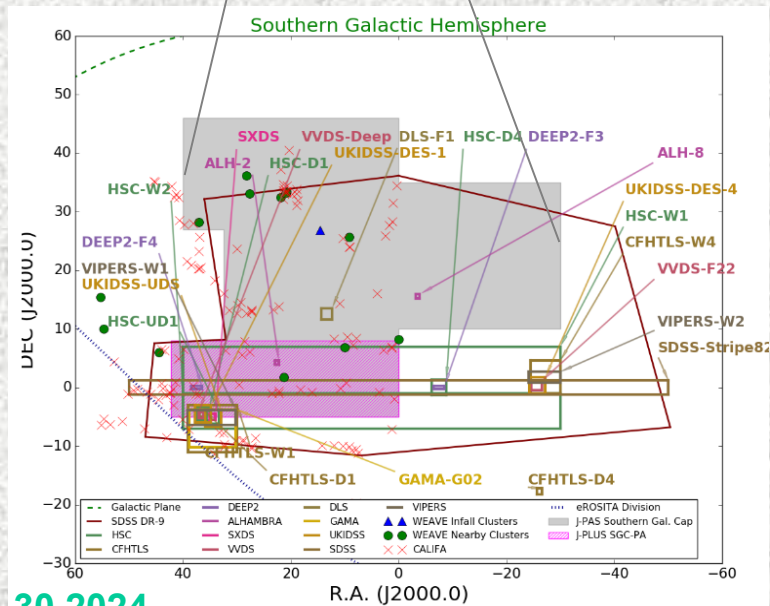
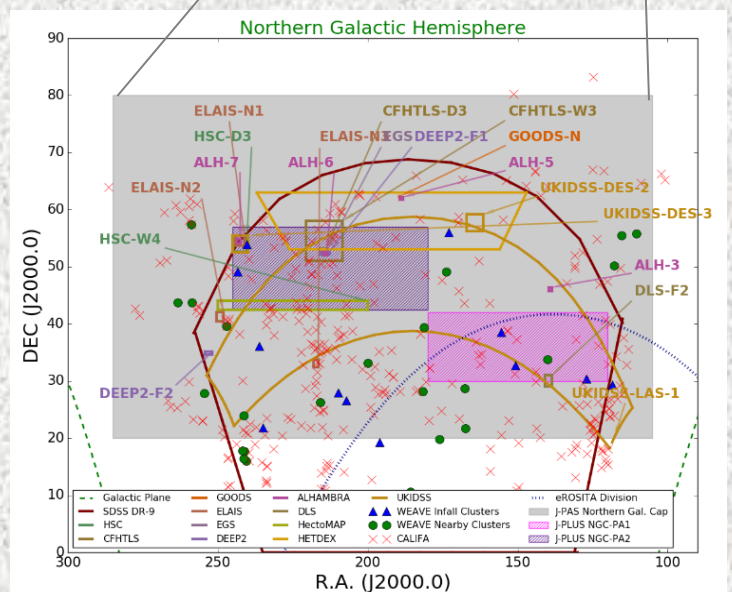
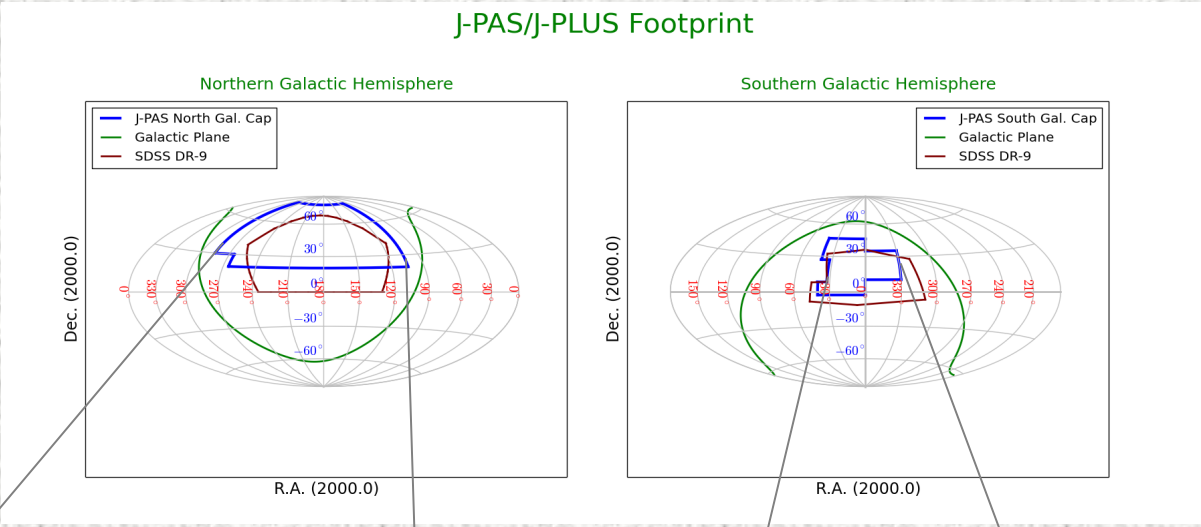


Footprint



~8,500 sq.deg

J-PAS/J-PLUS Footprint

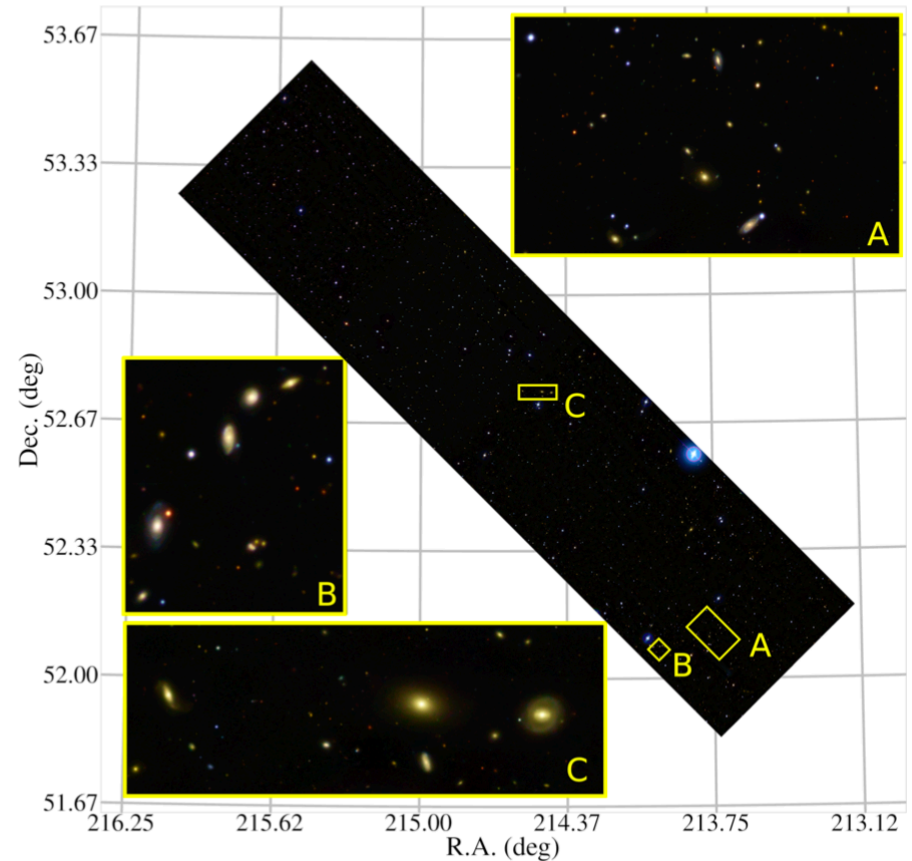
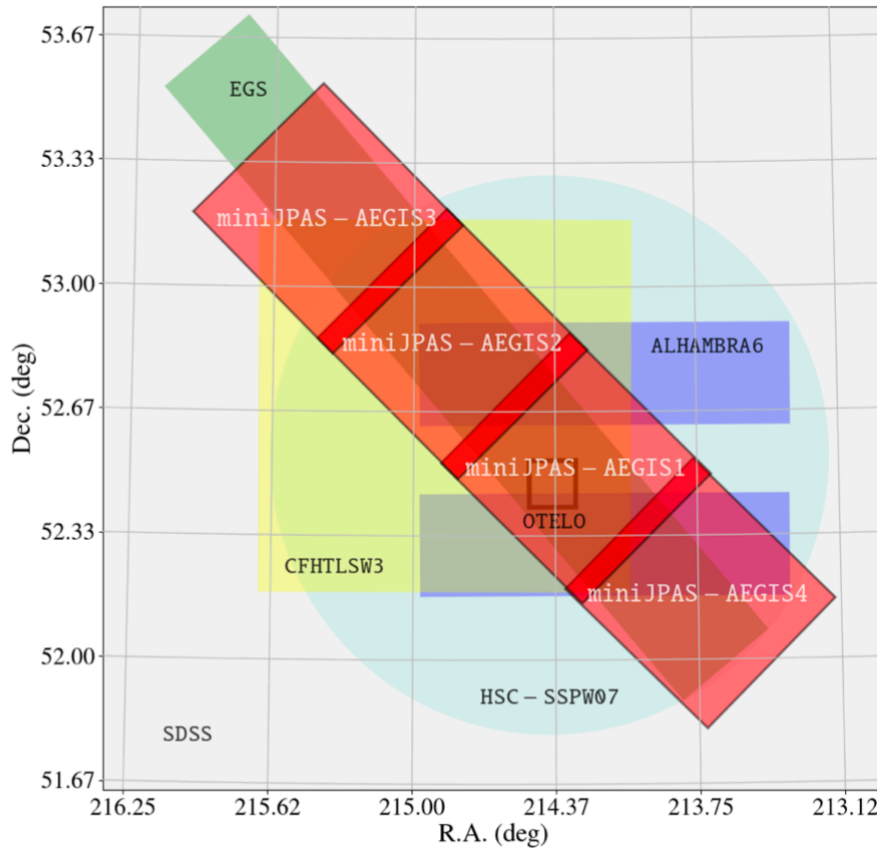


The first areas covered by J-PAS: miniJPAS and J-NEP

miniJPAS AEGIS fields (~1 sq.deg)

Bonoli + J-PAS Collab. 2021

A&A proofs: manuscript no. mini_jpas



miniJPAS data publicly available!
<https://archive.cefa.es/catalogues>

The miniJPAS survey: a preview of the Universe in 56 colours

S. Bonoli^{1,2,3*}, A. Marín-Franch⁴, J. Varela⁴, H. Vázquez Ramió⁴, L. R. Abramo⁵, A. J. Cenarro⁴, R. A. Dupke^{6,31,32**}, J. M. Vílchez⁷, D. Cristóbal-Hornillos¹, R. M. González Delgado⁷, C. Hernández-Monteagudo⁴, C. López-Sanjuan⁴, D. J. Muniesa¹, T. Civera¹, A. Ederoclite¹³, A. Hernán-Caballero¹, V. Marra⁸, P.O. Baqui⁸, A. Cortesi²⁰, E.S. Cypriano¹³, S. Daflon⁶, A. L. de Amorim²⁴, L. A. Díaz-García¹¹, J. M. Diego¹², G. Martínez-Solauche⁷, E. Pérez⁷, V. M. Placco^{17,18}, F. Prada⁷, C. Queiroz⁵, J. Alcaniz^{6,45}, A. Alvarez-Candal^{22,6}, J. Cepa^{41,42}, A. L. Maroto²³, F. Roig⁶, B. B. Siffert¹⁵, K. Taylor³⁴, N. Benitez⁷, M. Moles^{1,7}, L. Sodr e Jr.¹³, S. Carneiro¹⁰, C. Mendes de Oliveira¹³, E. Abdalla⁵, R. E. Angulo^{2,3}, M. Aparicio Resco²³, A. Balaguera-Antol nez^{41,42}, F. J. Ballesteros⁵⁰, D. Brito-Silva¹³, T. Broadhurst^{2,3,40}, E. R. Carrasco⁴⁸, T. Castro^{25,26,27,28}, R. Cid Fernandes²⁴, P. Coelho¹³, R. B. de Melo^{6,32}, L. Doubrawa¹³, A. Fernandez-Soto^{12,39}, F. Ferrari¹⁴, A. Finoguenov³⁷, R. Garc a-Benito⁷, J. Iglesias-P ramo⁷, Y. Jim nez-Teja⁷, F. S. Kitaura^{41,42}, J. Laur²⁹, P. A. A. Lopes²⁰, G. Lucatelli¹⁴, V. J. Mart nez^{39,50,51}, M. Maturi^{35,36}, M. Quartin^{19,20}, C. Pigozzo¹⁰, J. E. Rodr guez-Mart n⁷, V. Salzano⁵⁸, A. Tamm²⁹, E. Tempel²⁹, K. Umetsu¹¹, L. Valdivielso¹, R. von Martens⁶, A. Zitrin¹⁶, M. C. D az-Mart n¹, G. L pez-Alegre¹, A. L pez-Sainz¹, A. Yanes-D az¹, F. Rueda-Teruel¹, S. Rueda-Teruel¹, J. Abril Iba nez^{1,30}, J.L. Ant n Bravo¹, R. Bello Ferrer¹, S. Bielsa¹, J. M. Casino¹, J. Castillo¹, S. Chueca¹, L. Cuesta¹, J. Garzar n Calderaro¹, R. Iglesias-Marzoa¹, C.  niguez¹, J. L. Lamadrid Gutierrez¹, F. Lopez-Martinez¹, D. Lozano-P rez¹, N. Ma cas Sacrist n¹, E. L. Molina-Iba nez¹, A. Moreno-Signes¹, S. Rodr guez Llano¹, M. Royo Navarro¹, V. Tilve Rua¹, U. Andrade⁶, E. J. Alfaro⁷, S. Akras¹⁴, P. Arnalte-Mur^{50,51}, B. Ascaso⁵⁵, C. E. Barbosa¹³, J. Beltr n Jim nez⁶³, M. Benetti^{59,60}, C. A. P. Bengaly⁶, A. Bernui⁶, J. J. Blanco-Pillado^{3,40}, M. Borges Fernandes⁶, J. N. Bregman³¹, G. Bruzual⁵³, G. Calderone²⁶, J. M. Carvano⁶, L. Casarini⁹, A. L Chies-Santos⁴⁵, G. Coutinho de Carvalho⁴⁹, P. Dimauro⁶, S. Duarte Puertas⁷, D. Figueruelo⁶³, J. I. Gonz lez-Serrano¹², M. A. Guerrero⁷, S. Gurung-L pez^{1,47}, D. Herranz¹², M. Huertas-Company^{41,42,43,44}, J. A. Irwin³², D. Izquierdo-Villalba¹, A. Kanaan²⁴, C. Kehrig⁷, C. C. Kirkpatrick³⁷, J. Lim⁵⁶, A. R. Lopes⁶, R. Lopes de Oliveira^{9,6}, A. Marcos-Caballero⁴⁰, D. Mart nez-Delgado⁷, E. Mart nez-Gonz lez¹², G. Mart nez-Somonte^{12,62}, N. Oliveira⁶, A. A. Orsi¹, R. A. Overzier⁶, M. Penna-Lima³³, R. R. R. Reis^{19,20}, D. Spinosa¹, S. Tsujikawa⁶¹, P. Vielva¹², A. Z. Vitorelli¹³, J. Q. Xia²¹, H. B. Yuan²¹, A. Arroyo-Polonio⁷, M. L. L. Dantas¹³, C. A. Galarza⁶, D. R. Gonalves²⁰, R. S. Gonalves⁶, J. E. Gonzalez^{6,45}, A. H. Gonzalez⁵⁴, N. Greisel¹, R. G. Landim³⁸, D. Lazzaro⁶, G. Magris⁵², R. Monteiro-Oliveira¹³, C.B. Pereira⁶, M. J. Rebouas⁵⁷, J. M. Rodriguez-Espinosa⁴², S. Santos da Costa⁶, E. Telles⁶

(Affiliations can be found after the references)

July 10, 2020

The miniJPAS depth and FWHM values

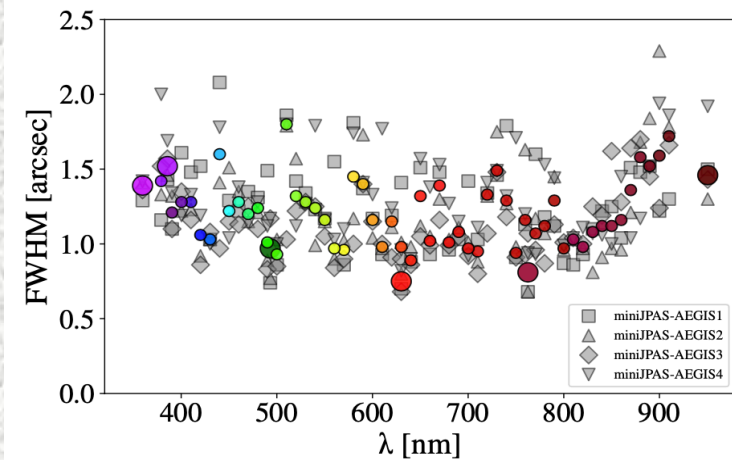


Fig. 5: Statistics of the PSF FWHM. The coloured symbols represent the average values for each filter, while the gray ones are the value for each pointing. The larger symbols indicate the the FWHM of the the broad bands.

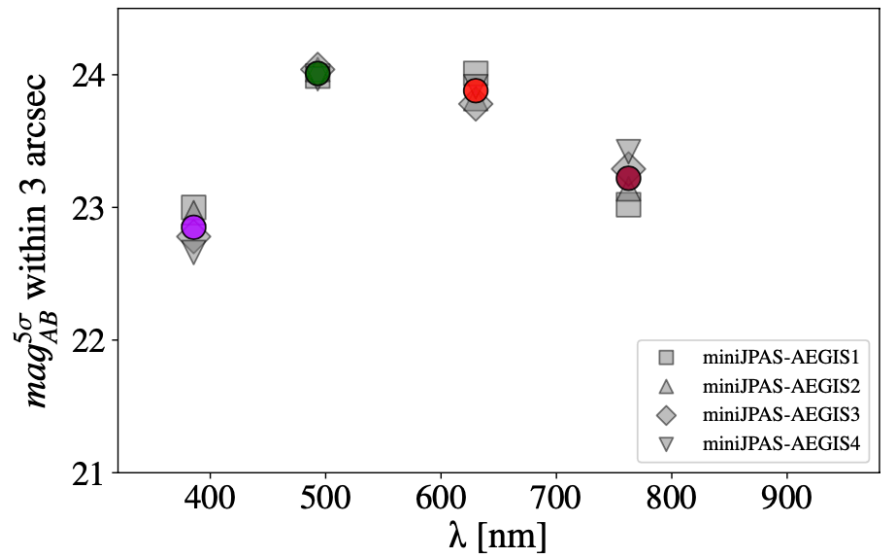
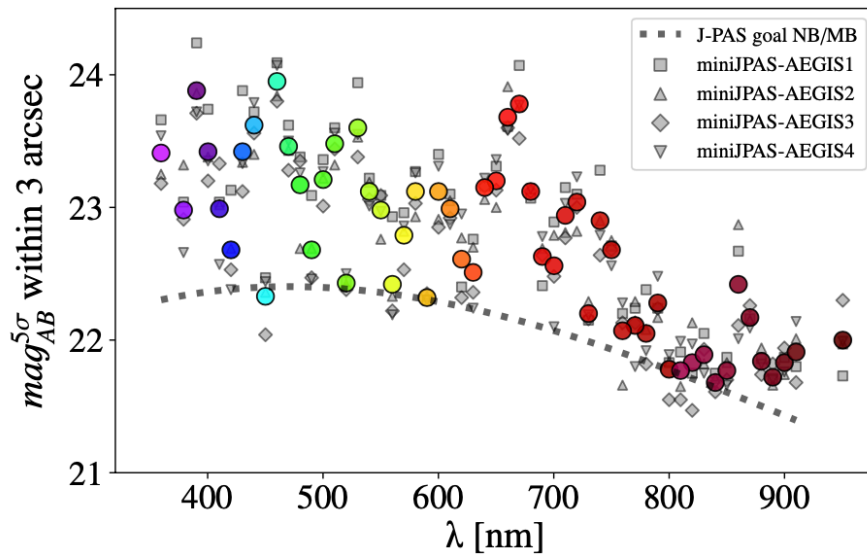
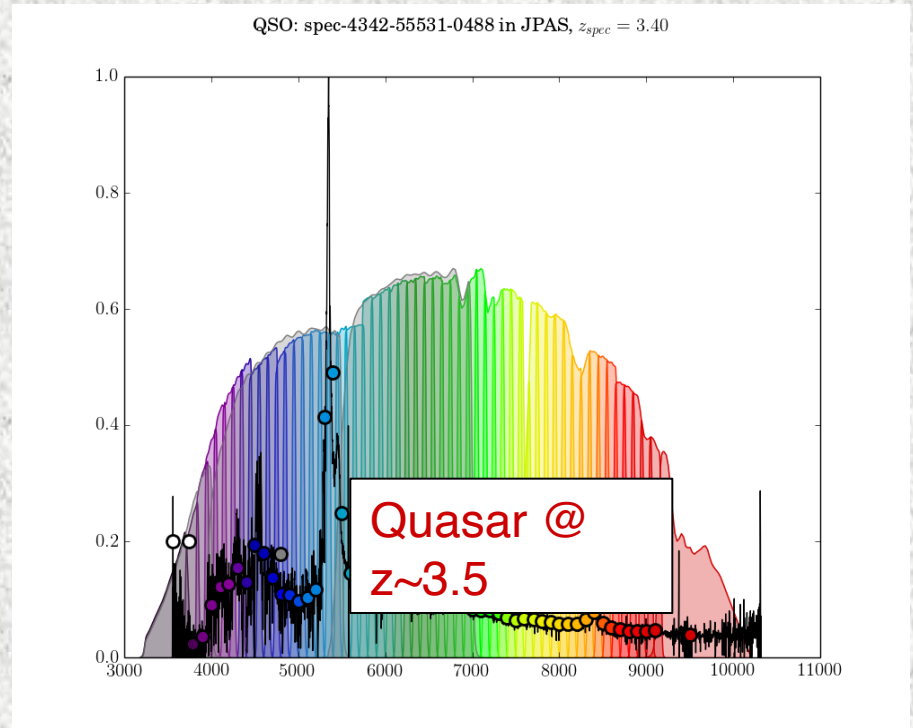
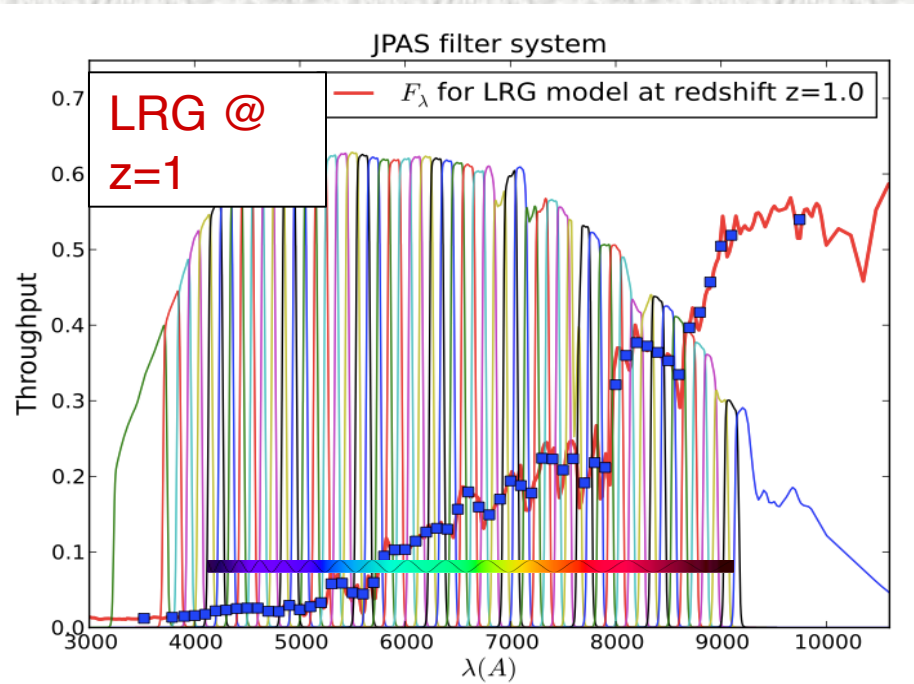
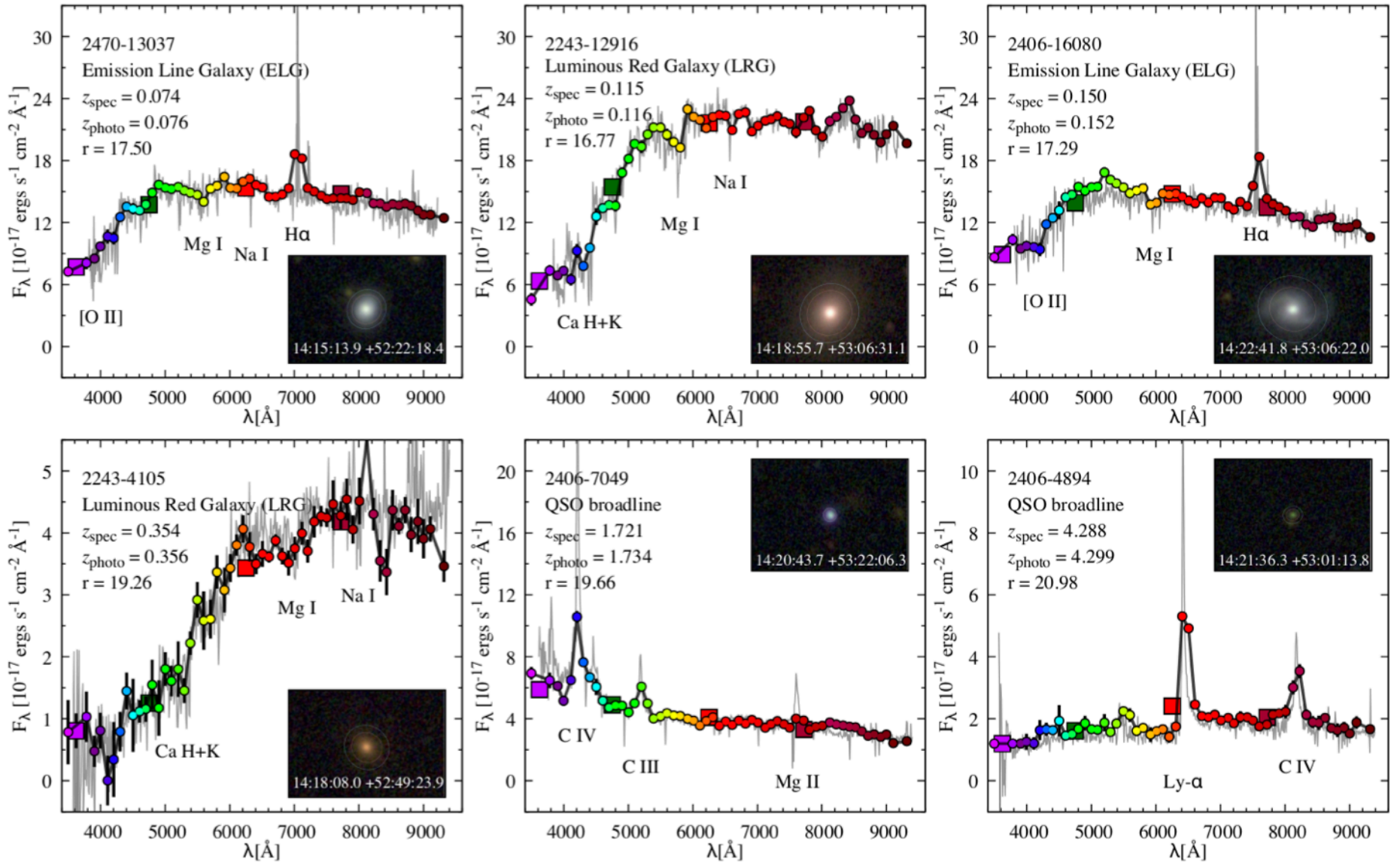


Fig. 4: Estimated depths (5σ at 3 arcsec aperture), computed from the noise in each tile, for the narrow bands (left) and broad bands (right). The coloured symbols show the average values for each filter, while the gray ones are the values for the co-added images of each pointing. For the narrow bands, the dashed gray line indicates the approximate targeted minimum depth, as defined in [Benítez et al. \(2014\)](#).





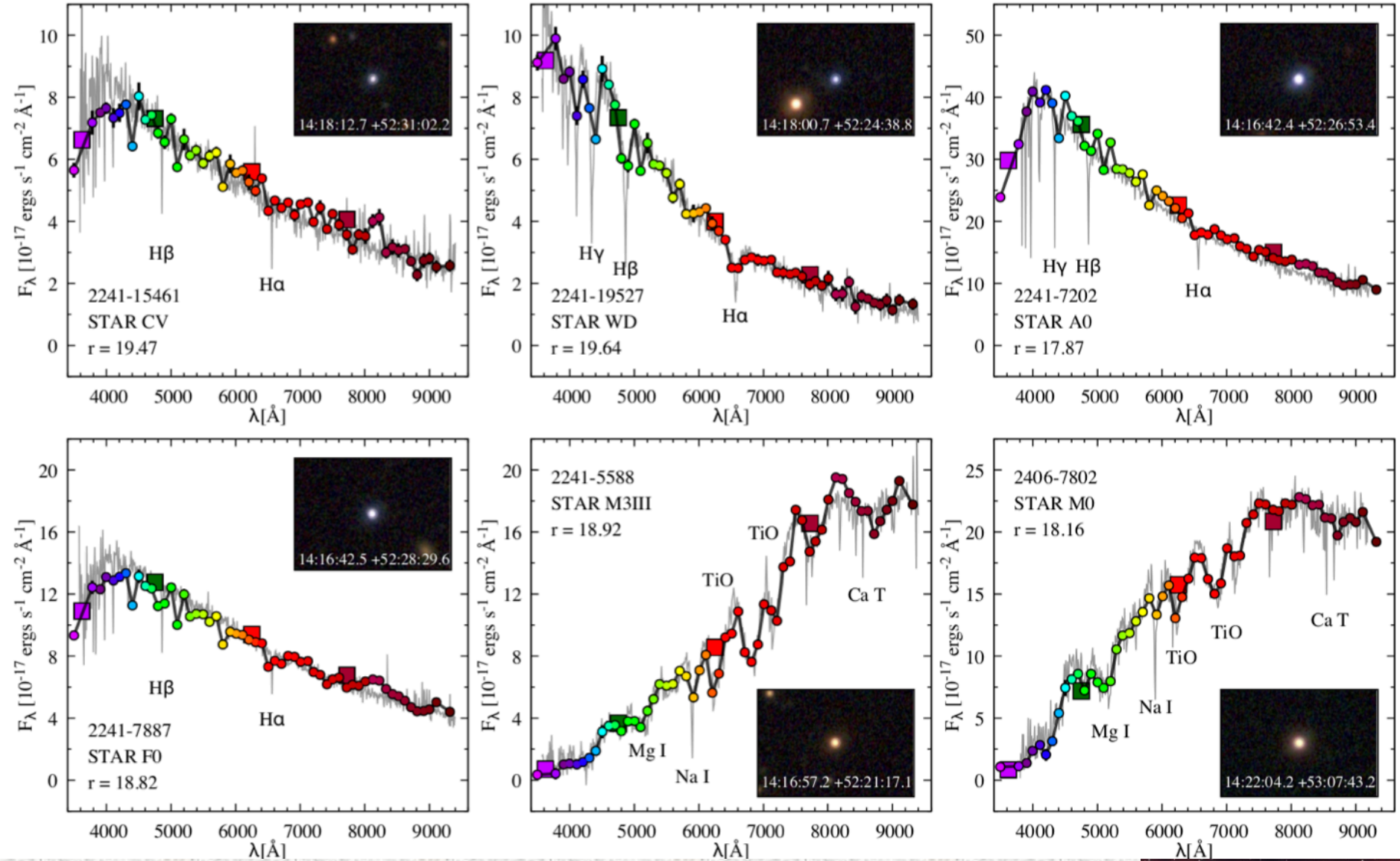
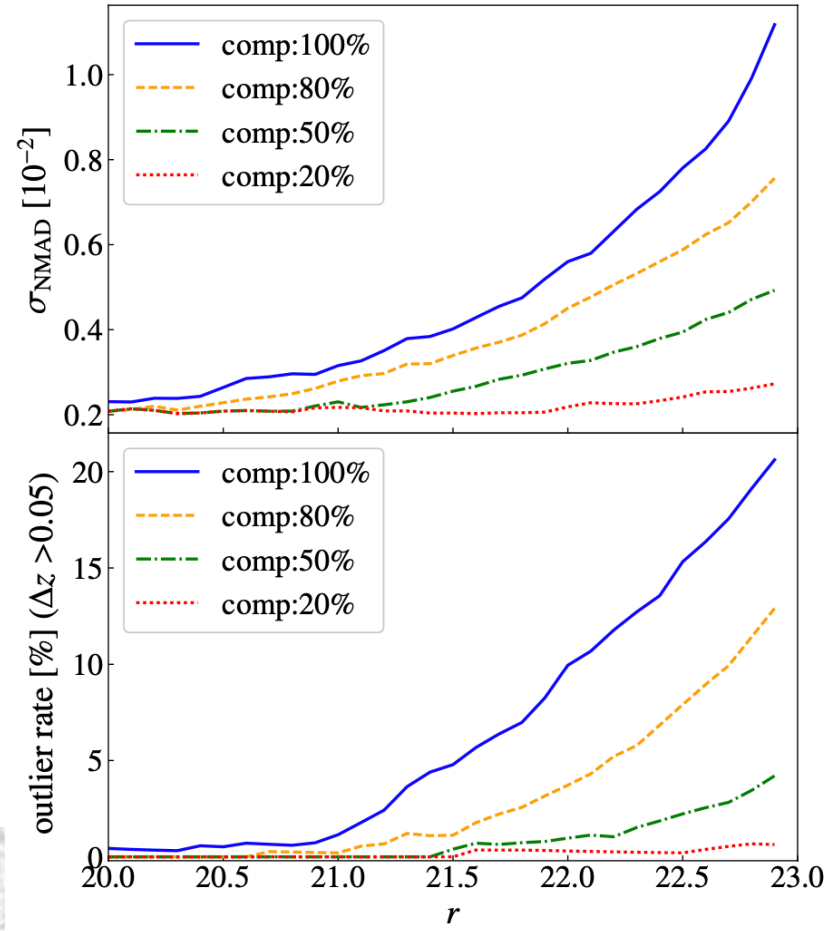
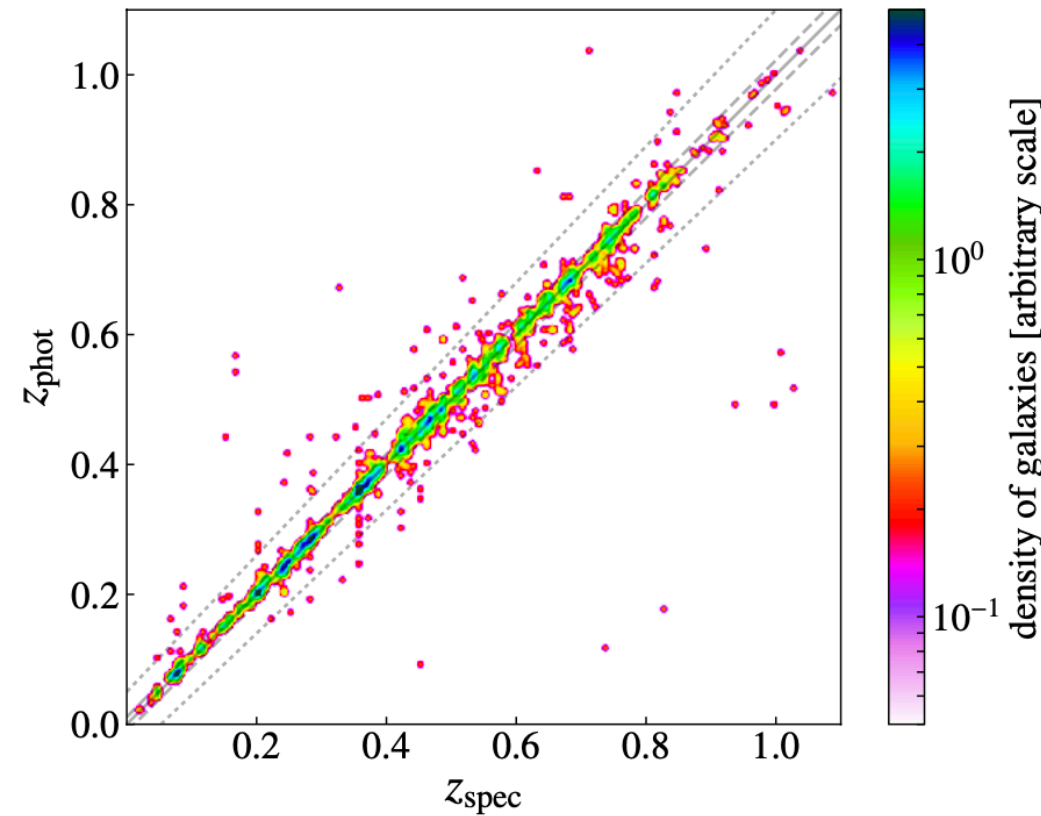


Photo-z precision as
good as $0.003(1+z)$

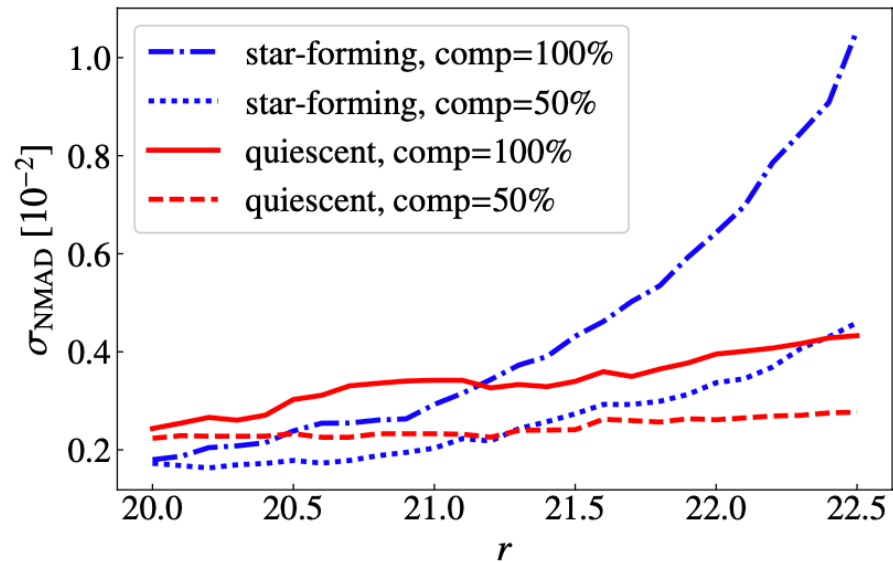
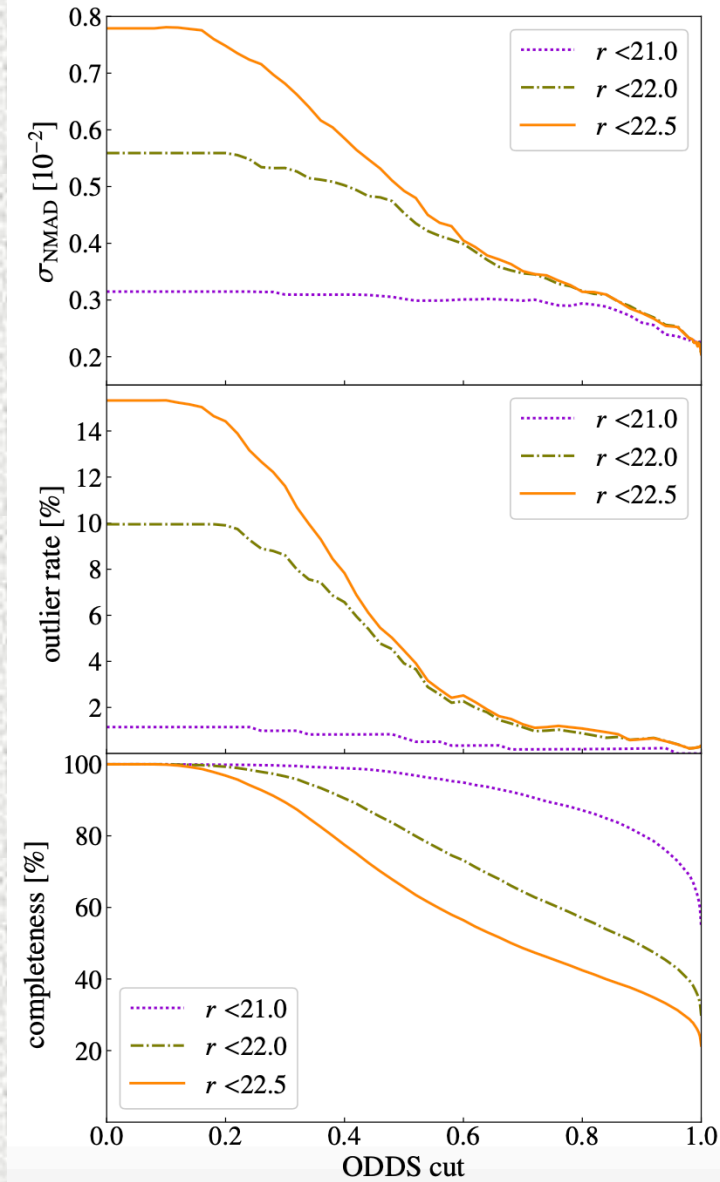
Photo-z precision as good as $0.003(1+z)$



Hernán-Caballero +J-PAS, 2021,2023

Photo-z precision as good as $0.003(1+z)$

Hernán-Caballero + J-PAS, 2021, 2023

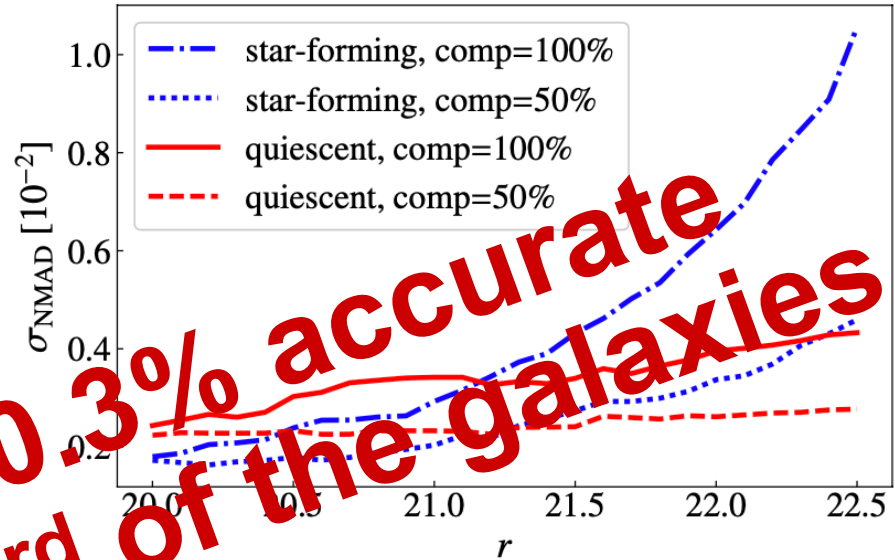
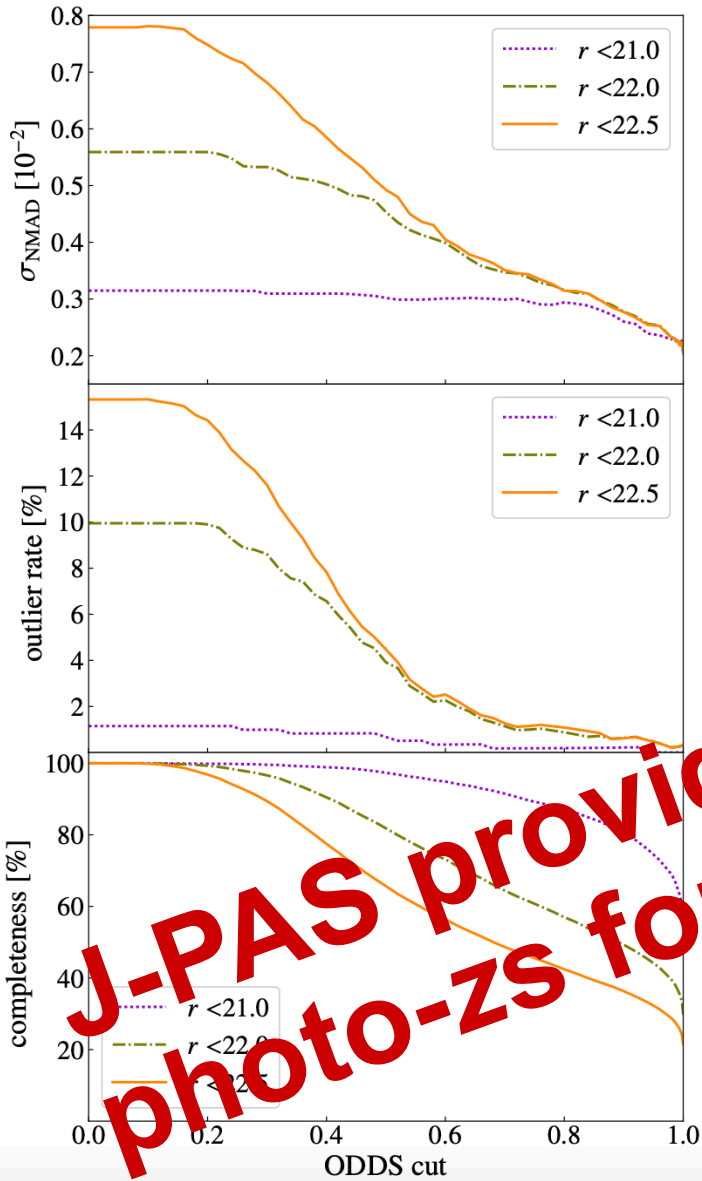


$$\text{odds} = \int_{z_{\text{phot}}-d}^{z_{\text{phot}}+d} P(z) dz, \quad d = 0.03(1 + z_{\text{phot}})$$

The **odds** parameter **captures** the precision of the photo-z *independently* of galaxy's magnitude or type: selections must be done in **odds**

Photo-z precision as good as $0.003(1+z)$

Hernán-Caballero +J-PAS, 2021,2023



J-PAS provides ~0.3% accurate photo-zs for ~1/3rd of the galaxies

$$odds = \int_{z_{phot}-d}^{z_{phot}+d} P(z) dz, \quad d = 0.03(1 + z_{phot})$$

The **odds** parameter **captures** the precision of the photo-z **independently** of galaxy's magnitude or type: selections must be done in **odds**

J-PAS LSS Cosmological probes of Dark Energy

QSO science

- ~1 M QSOs with photo-z precision of 0.3% or better SNIa
- MoU with WEAVE-QSO to conduct Ly- α forest science using WEAVE MOS.

- 90M galaxies (LRG, ELG) with photo-z precision of 0.3%
- ks LAE

Clustering

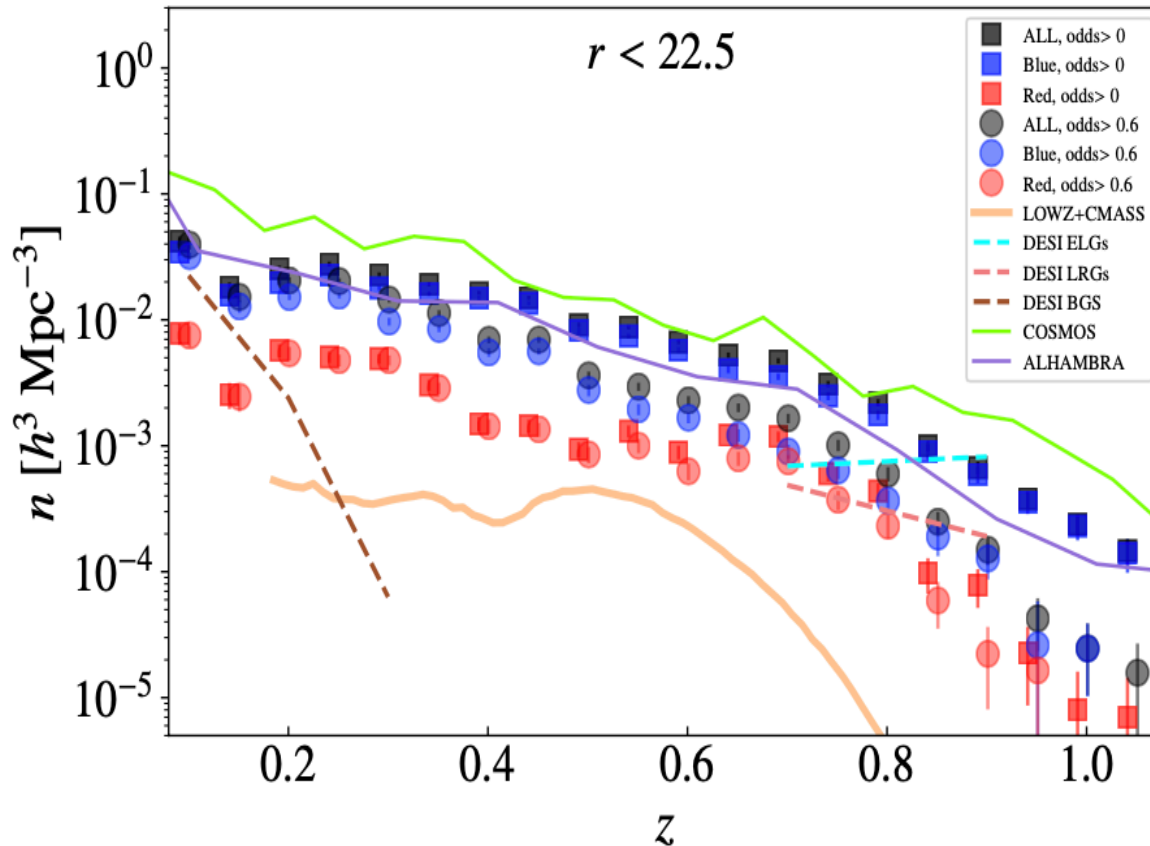
Clusters

- 700k clusters with more than 10 members – down to ~few $\times 10^{13} M_{\odot}$
- Combine lensing and optical richness for mass calibration

- Optimization of BB observations in the best nights
- Redshift precision for lenses and background galaxies

Lensing

LSS in miniJPAS

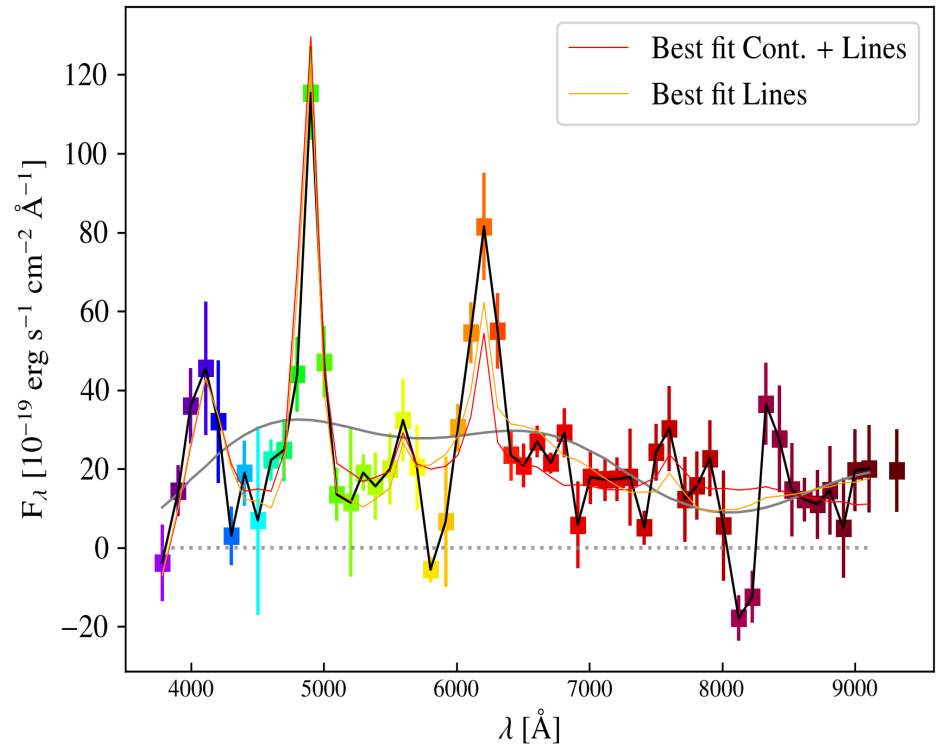
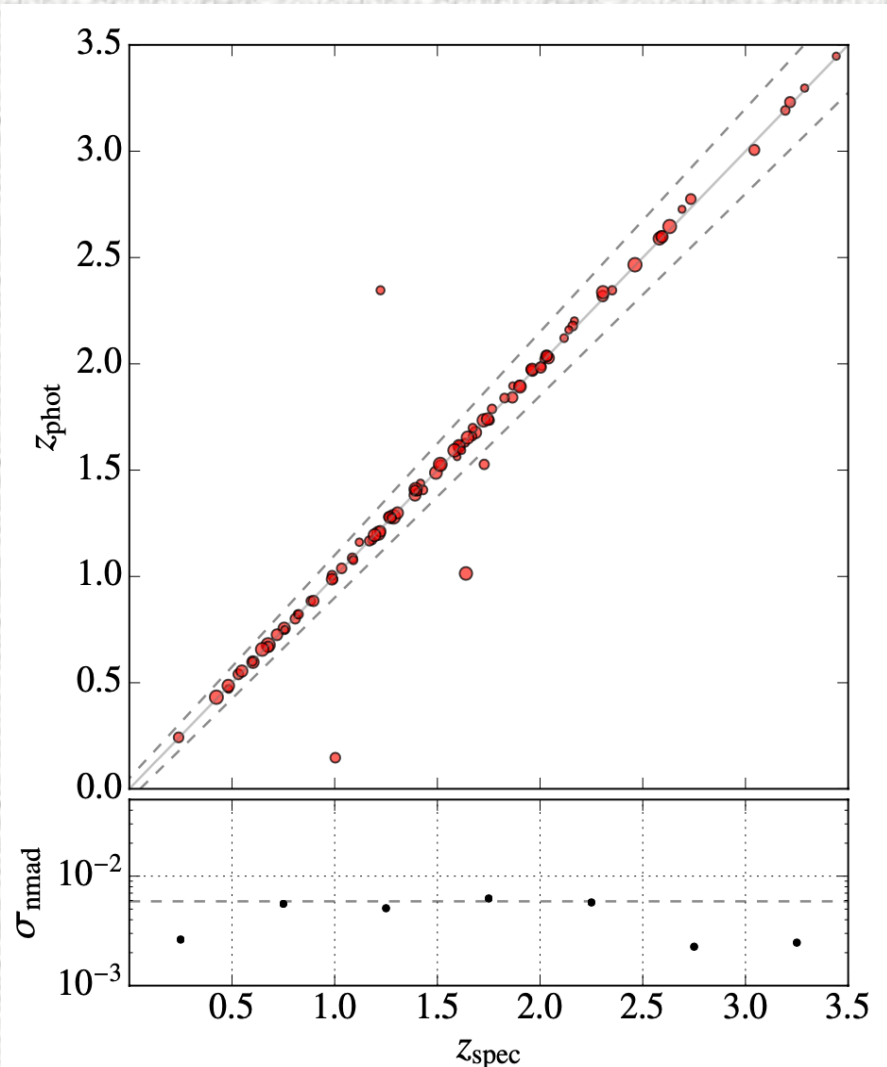


- **High quality** photo-zs for all red galaxies up to $z \sim 0.9$
- **High quality** photo-zs for a large fraction of blue galaxies up to $z \sim 0.9$
- **Multi-tracer** science enabled in a very wide redshift range $z \sim [0, 1]$
- Clustering science cases augmented after the inclusion of the **J-PAS QSO** population (~ 1.5 M) sampling the redshift interval $z \sim [1, 3.5]$
- Further science cases after obtaining spectra with **WEAVE-QSO**

QSOs in J-PAS

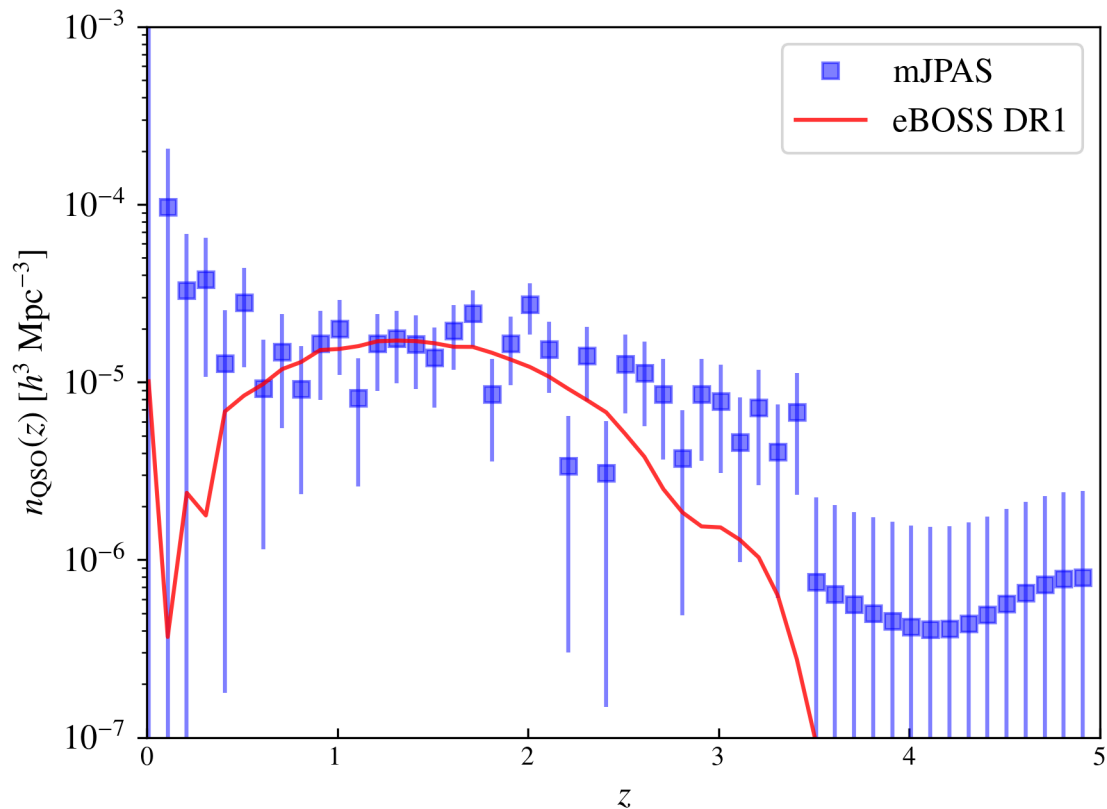
For **QSOs** we can recover very accurate and precise photo-z as well !!

ID= 2241, No= 5153, $\chi^2 = 5.69$, $r_{\text{JPAS}} = 22.396$, $z_{\text{phot}} = 3.00467 \pm 0.00401$

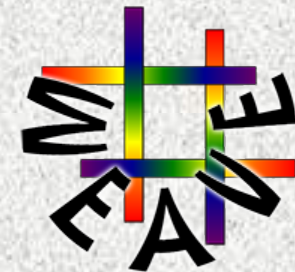


NUMBER DENSITY OF QSO CANDIDATES FROM miniJPAS

About 200 QSOs per sq.deg. ($r < 24$)



Ongoing program with **WEAVE QSO**: about **~700 sq.deg** per year of our **QSO candidates** will be covered with their fibers, enabling **Lyman-alpha science**



How's the impact of miniJPAS photo- z errors in clustering analysis?

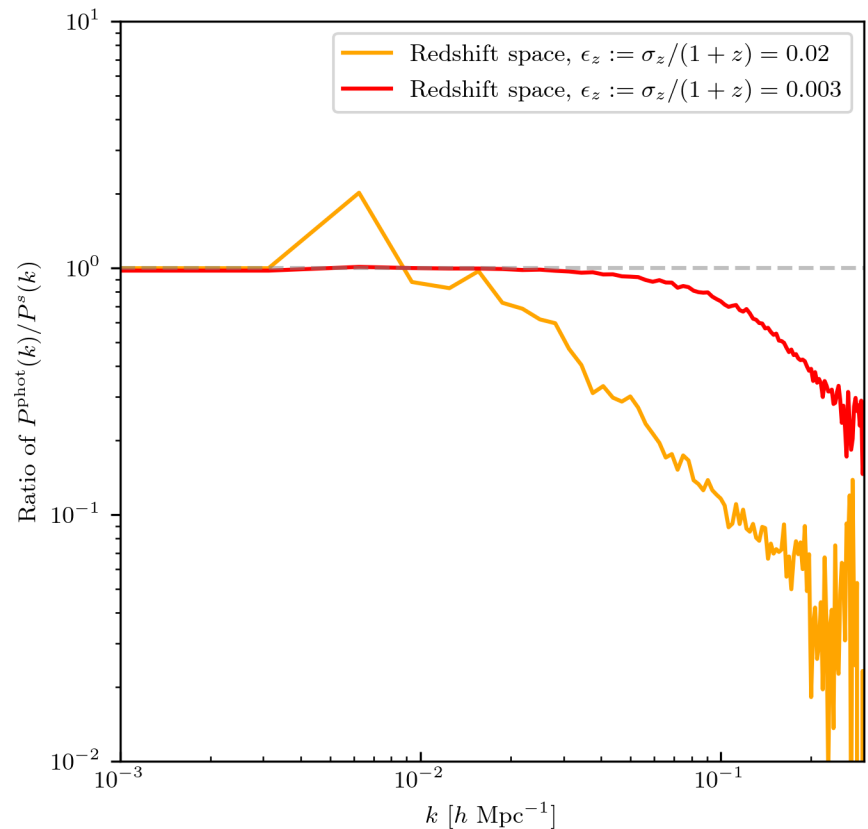
Projections of miniJPAS on LSS clustering

Ratio of $P_0(k)$ s:

$$P_{0,\text{photo}}(\mathbf{k}) / P_{0,\text{spec}}(\mathbf{k})$$

Obtained from **ideal, Gaussian Photo-z errors** at the targetted level of J-PAS

Forecasts on sensitivity of J-PAS to the **dark sector** (interacting dark matter and dark energy, exotic dark energy models) and **modified gravity** can be found in Salzano et al., 2021, Figueruelo et al. 2021, Aparicio-Resco et al. 2020, Costa et al. 2019.



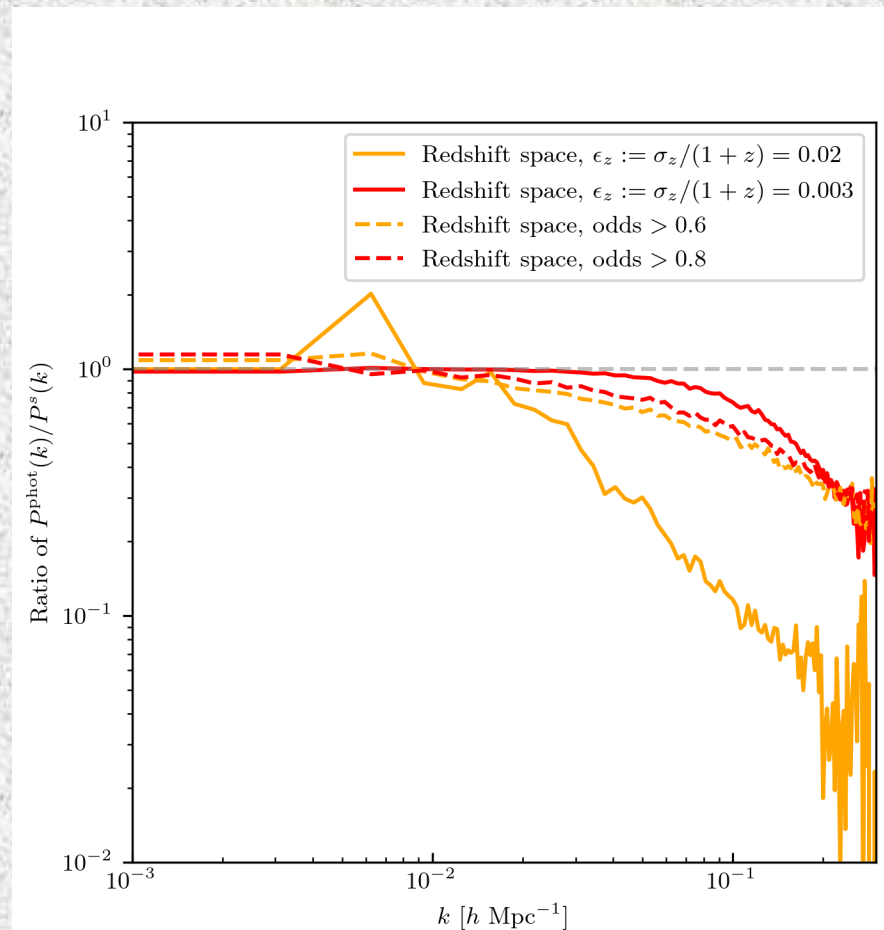
Projections of miniJPAS on LSS clustering

Ratio of $P_0(k)$ s:

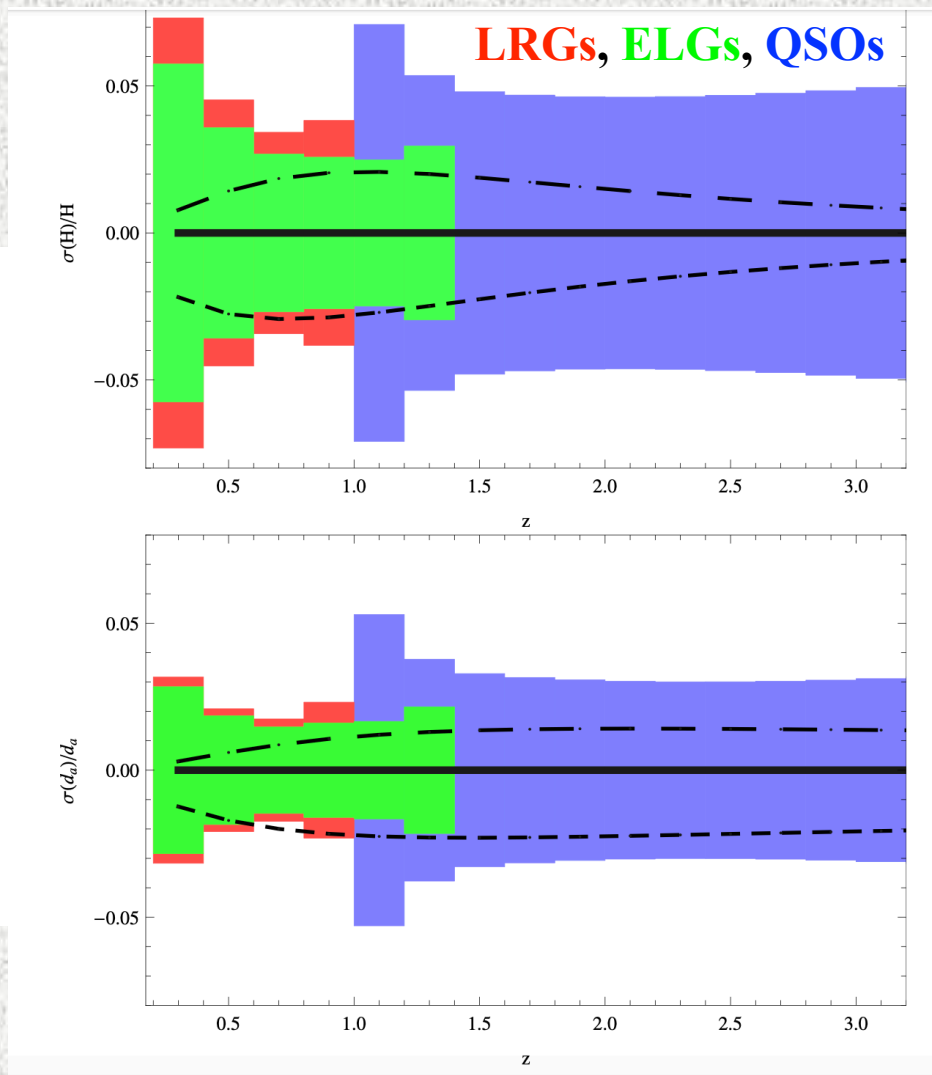
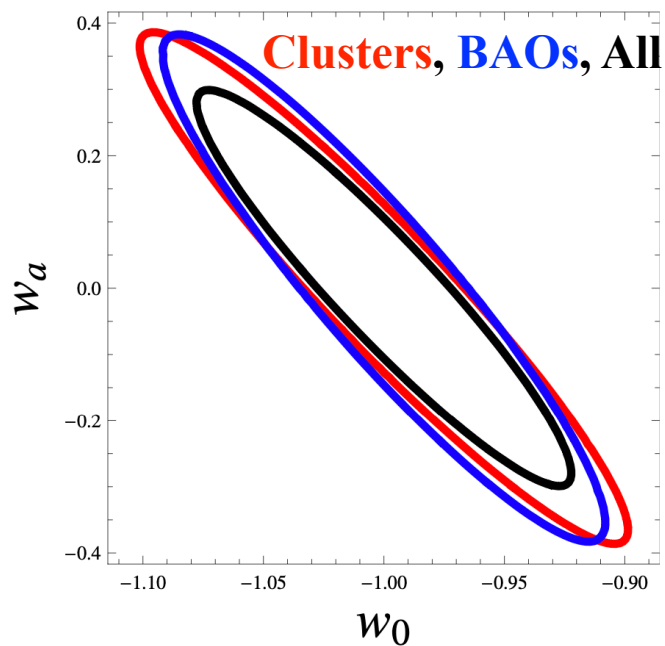
$$P_{0,\text{photo}}(k) / P_{0,\text{spec}}(k)$$

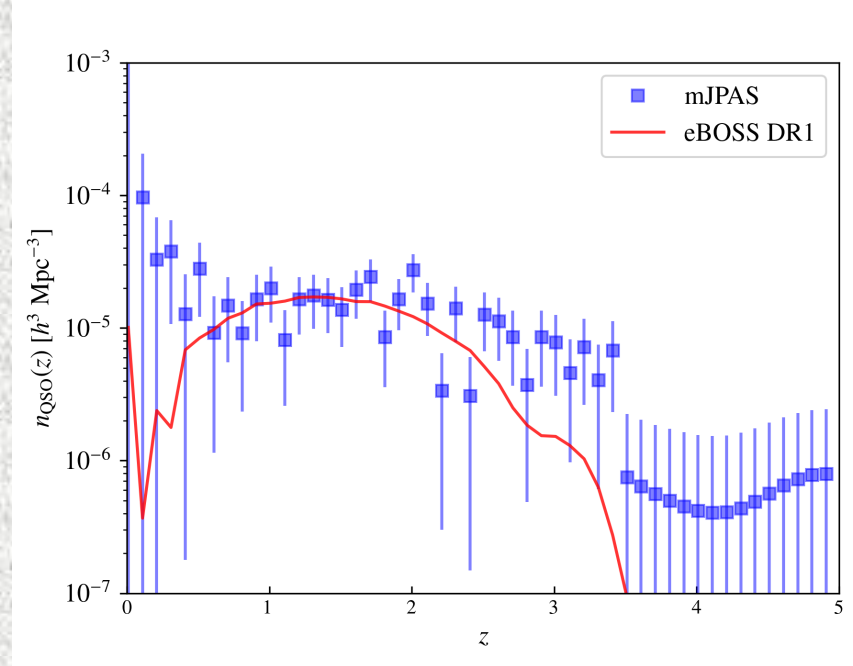
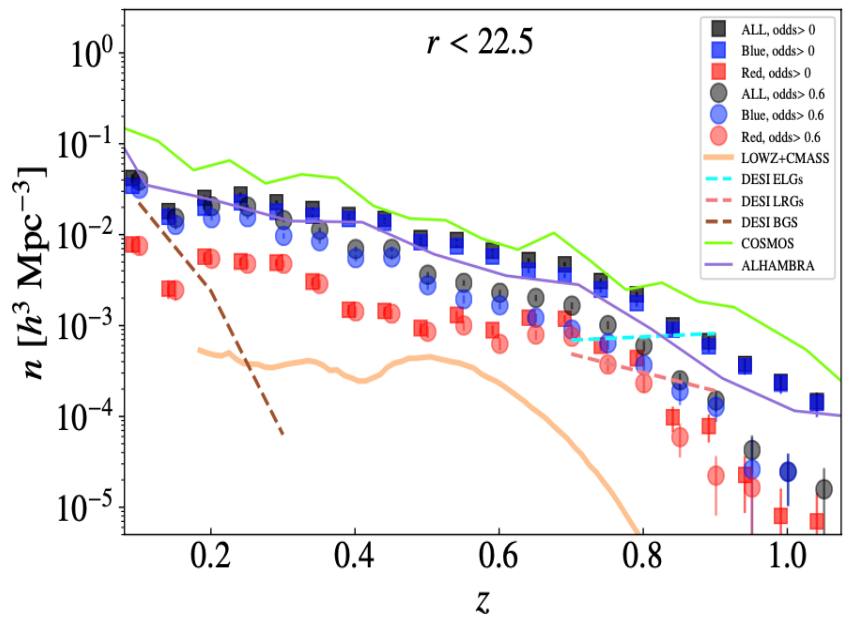
Obtained from **real photo-z PDFs** obtained from **miniJPAS** data

Forecasts on sensitivity of J-PAS to the **dark sector** (interacting dark matter and dark energy, exotic dark energy models) and **modified gravity** can be found in Salzano et al., 2021, Figueruelo et al. 2021, Aparicio-Resco et al. 2020, Costa et al. 2019.



J-PAS Fisher forecasts from Benitez+2014





- Forecasts show that J-PAS should recover practically all the information on **linear** cosmological scales on a very wide redshift range $z \in [0, 3.5]$.
- Measured miniJPAS galaxy and QSO number densities yield typically low(er) values for shot noise, **but**,
- The recovery of mildly to highly non-linear scales is compromised/ hampered by photo-z errors, deeming it challenging ...

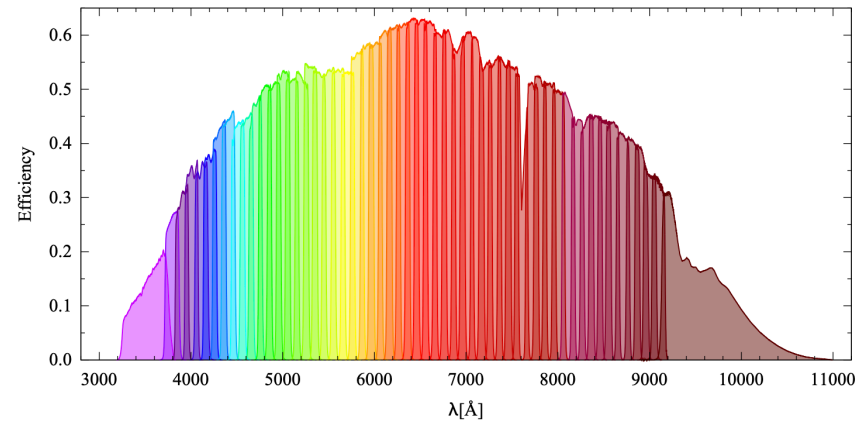
A low redshift example: tomographic analysis of J-PLUS

J-PLUS DR3 (~3,000 sq.deg)

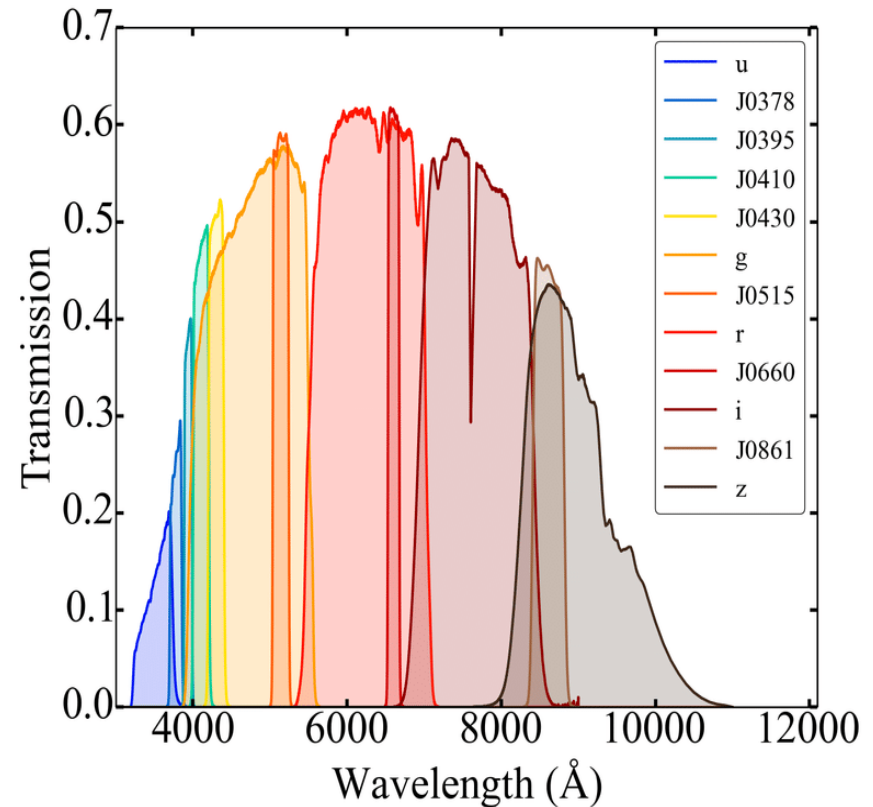
J-PAS

57 vs 12 filters ...

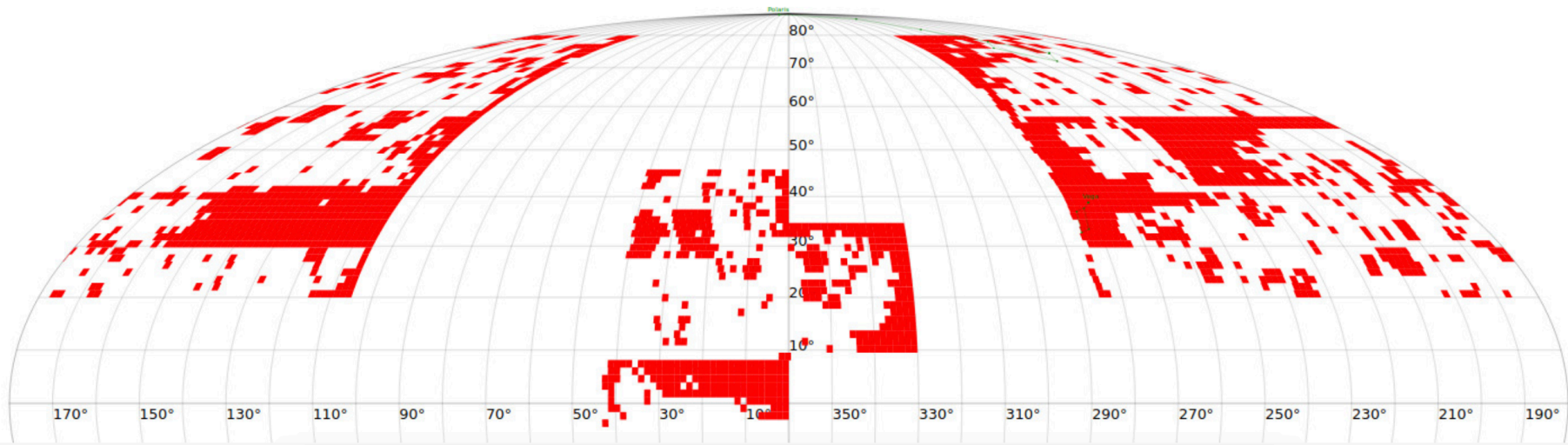
J-PLUS



measured transmission curves of the J-PAS filters. Effects of the CCD quantum efficiency, the entire optical system of the 1.5m telescope and sky absorption are included. The HTML color representation of each filter is provided in the table `miniJPAS.Filter`.



J-PLUS DR3 samples



Total area covered	3192 deg ² (~2881 deg ² after masking)
Image size	9500x9500 pixels (~2 deg ²)
Image pixel scale	0.555 arcsec
Total number of fields	1642
Number of objects in dual catalogue	~47.4 million (~29.8 million with MAG_AUTO(rSDSS)≤21)
Number of objects with estimations of photo-z (with their full PDFs)	~44.1 million
Number of detections in single catalogue	~338.4 million
Size of the database	~373 GB
Number of Single Frames	62310
Tile Images Total Size (compressed)	~962.1 GB
Single Frames Total Size (compressed)	~4.46 TB

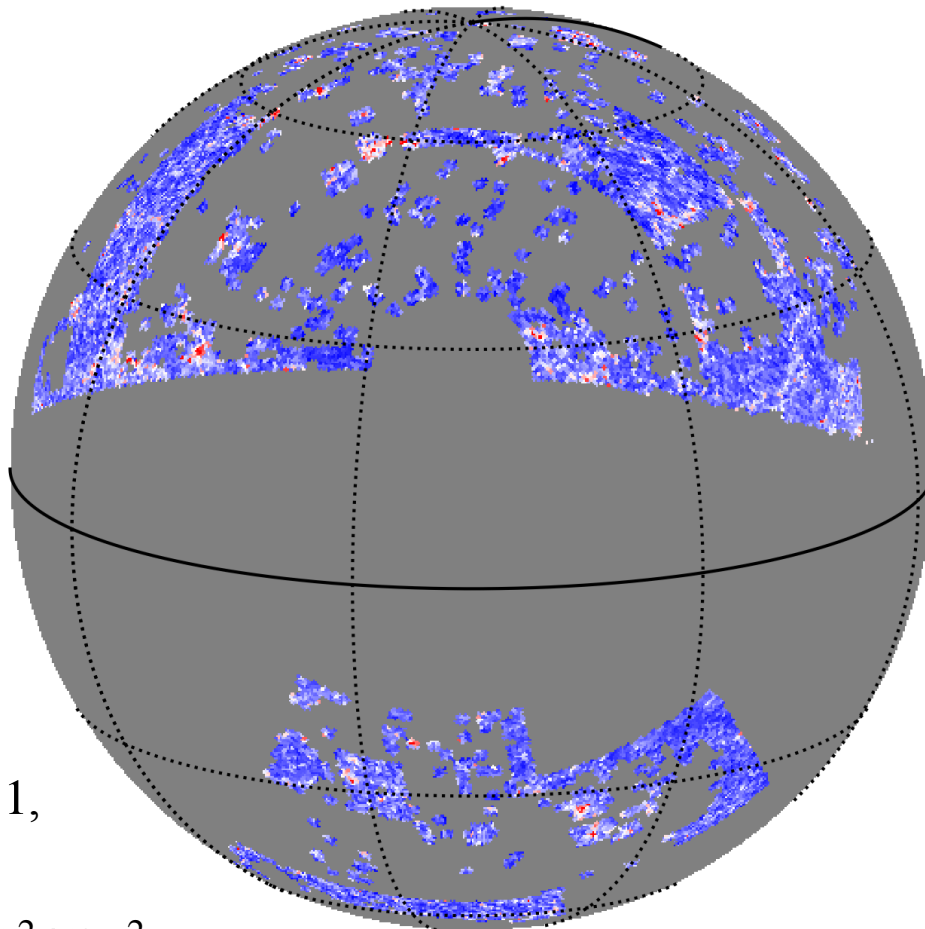
$odds > 0.8, r < 21, \sigma_{\text{Err}, z} \simeq 0.014$

XGBoost

2D clustering, source counts in footprint, angular density fluctuations (ADF)

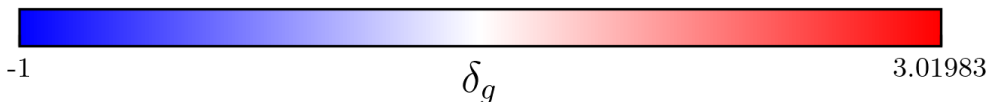
An example from **J-PLUS DR3**

POST ADF $z = 0.07, \sigma_z = 0.05$



$$\delta_g(\hat{\mathbf{n}}) = \frac{\sum_{j \in \hat{\mathbf{n}}} W_j}{\langle \sum_{i \in \hat{\mathbf{n}}} W_i \rangle_{\hat{\mathbf{n}}}} - 1,$$

$W_j := \exp[-(z_j - z_{\text{cen}})^2 / (2\sigma_z^2)]$, and z_{cen}, σ_z to be picked by the observer



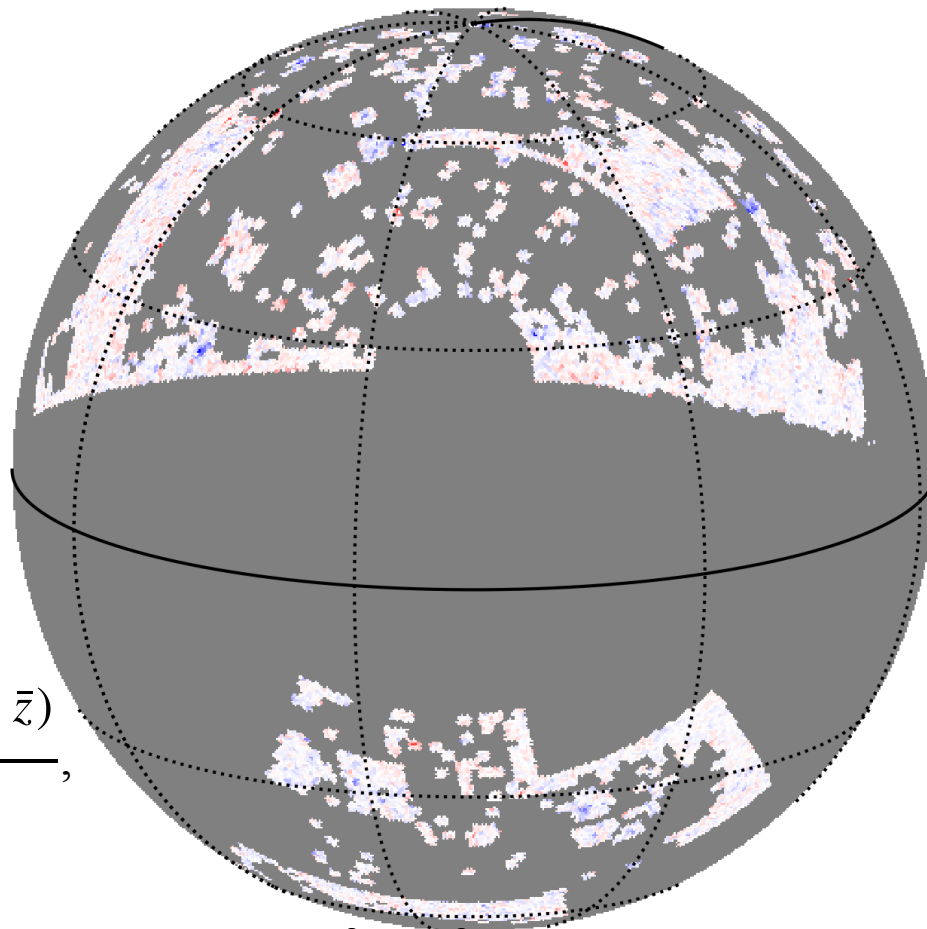
$odds > 0.8, r < 21, \sigma_{\text{Err}, z} \simeq 0.014$

XGBoost

Angular redshift fluctuations (ARF)
(Under any given redshift shell, a by construction much more Gaussian observable)

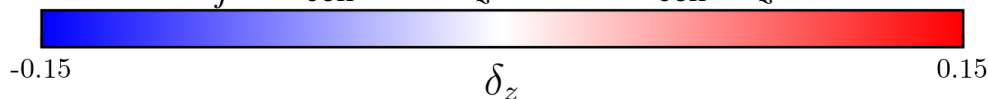
An example from **J-PLUS DR3**

PRE ARF, $z = 0.07, \sigma_z = 0.05$



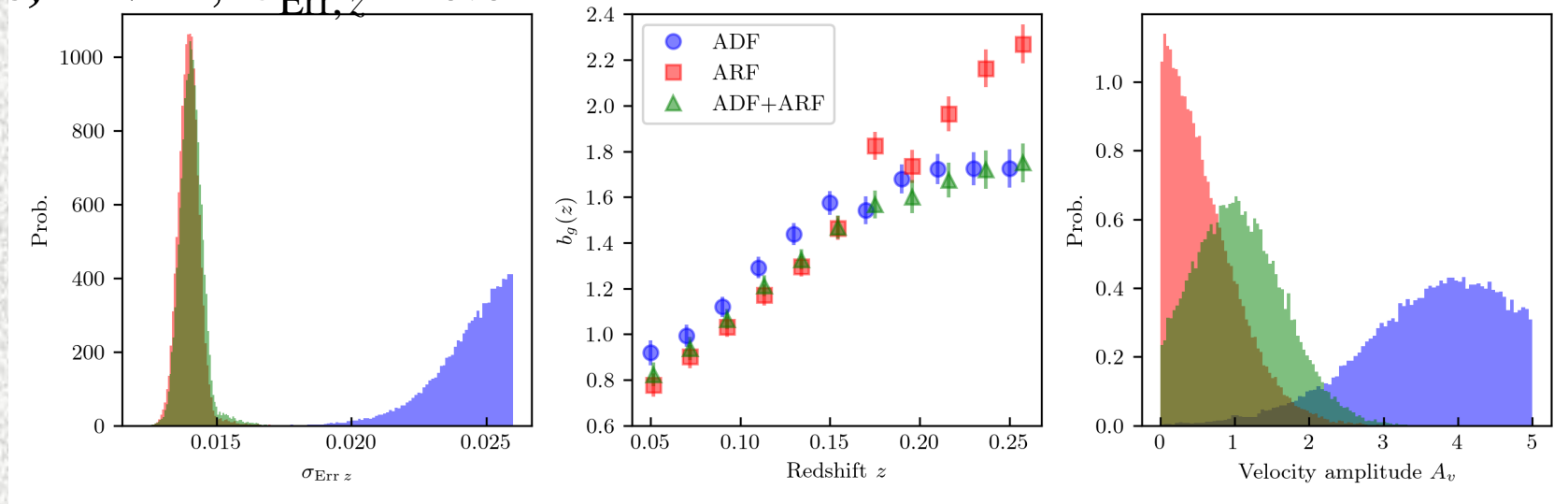
$$\delta z(\hat{\mathbf{n}}) = \frac{\sum_{j \in \hat{\mathbf{n}}} W_j (z_j - \bar{z})}{\langle \sum_{i \in \hat{\mathbf{n}}} W_i \rangle_{\hat{\mathbf{n}}}},$$

$$\bar{z} := \frac{\sum_j W_j z_j}{\sum_j W_j}; \quad W_j := \exp\left[-(z_j - z_{\text{cen}})^2 / (2\sigma_z^2)\right], \text{ and } z_{\text{cen}}, \sigma_z \text{ to be picked by the observer}$$

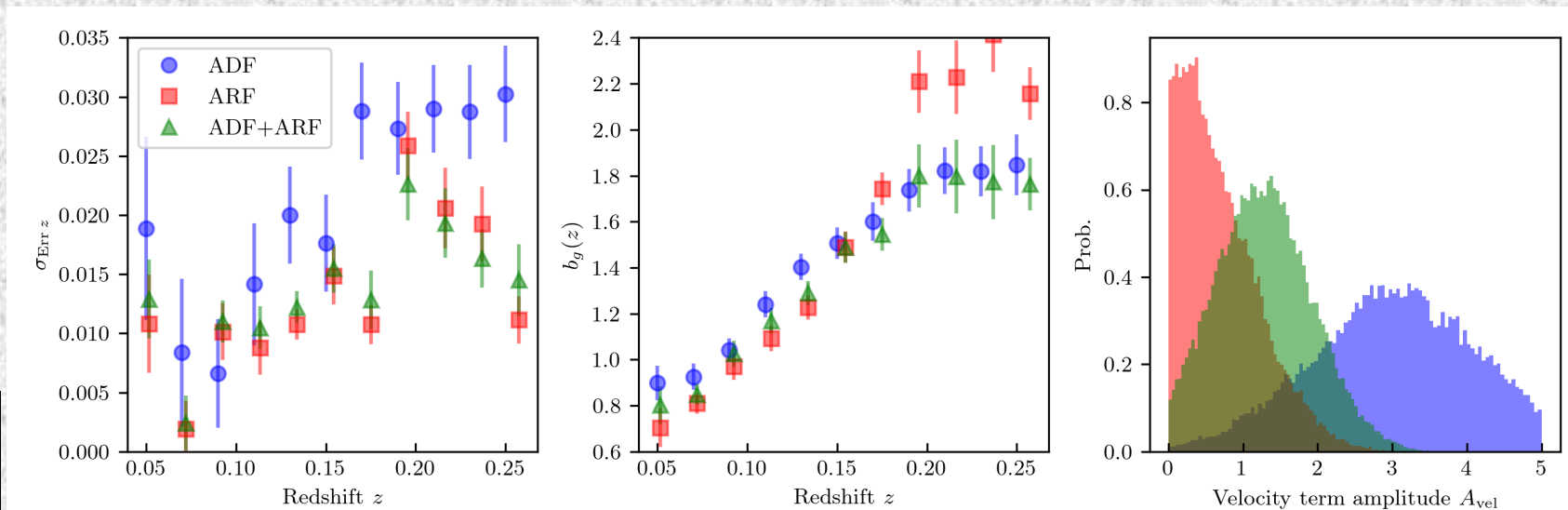


Unique σ_{Err} for all redshift shells: $\{\sigma_{\text{Err}}, b_{i=1, \text{nshells}}, \mathcal{A}_v\}$

$\text{odds} > 0.8, r < 21, \sigma_{\text{Err}, z} \simeq 0.014$

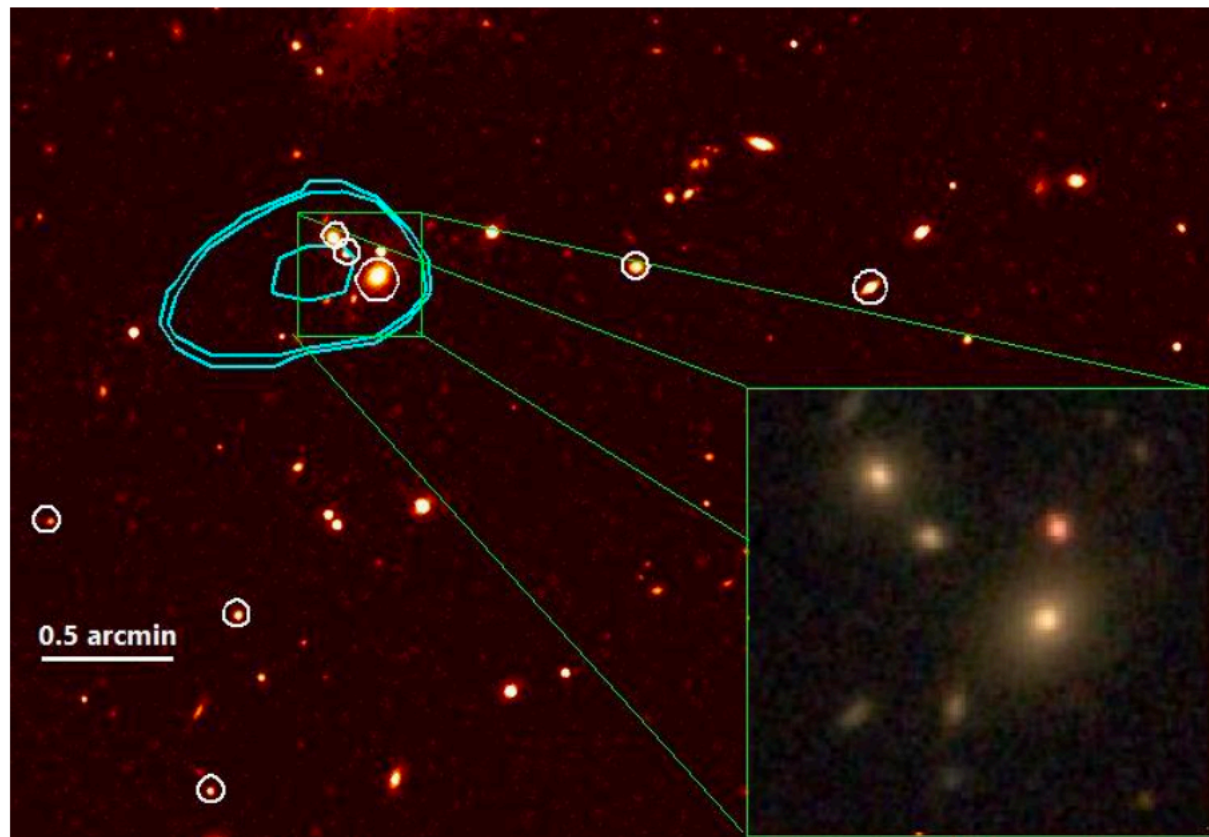


Different σ_{Err} for *each* redshift shells: $\{\sigma_{\text{Err}, i=1, \text{nshells}}, b_{i=1, \text{nshells}}, \mathcal{A}_v\}$



Clusters in miniJPAS

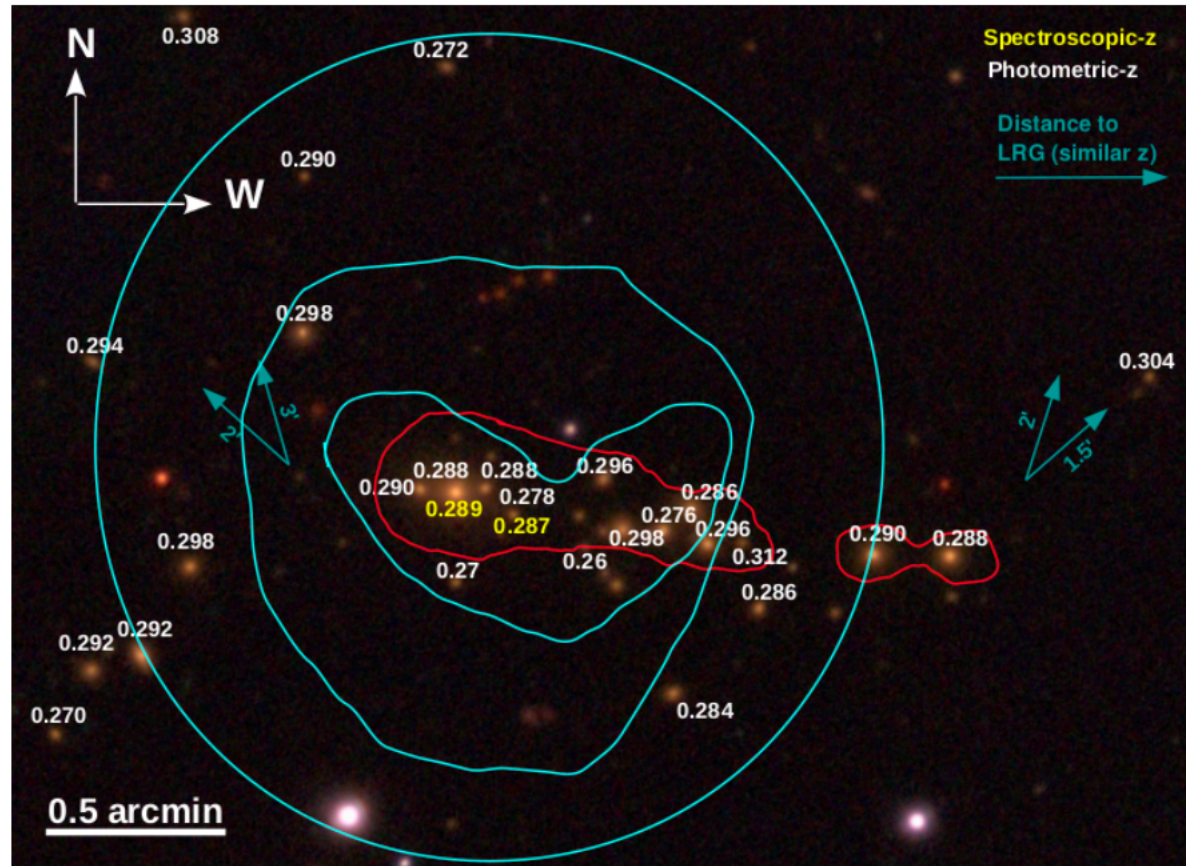
Clusters in miniJPAS



Currently two cluster finders in place:

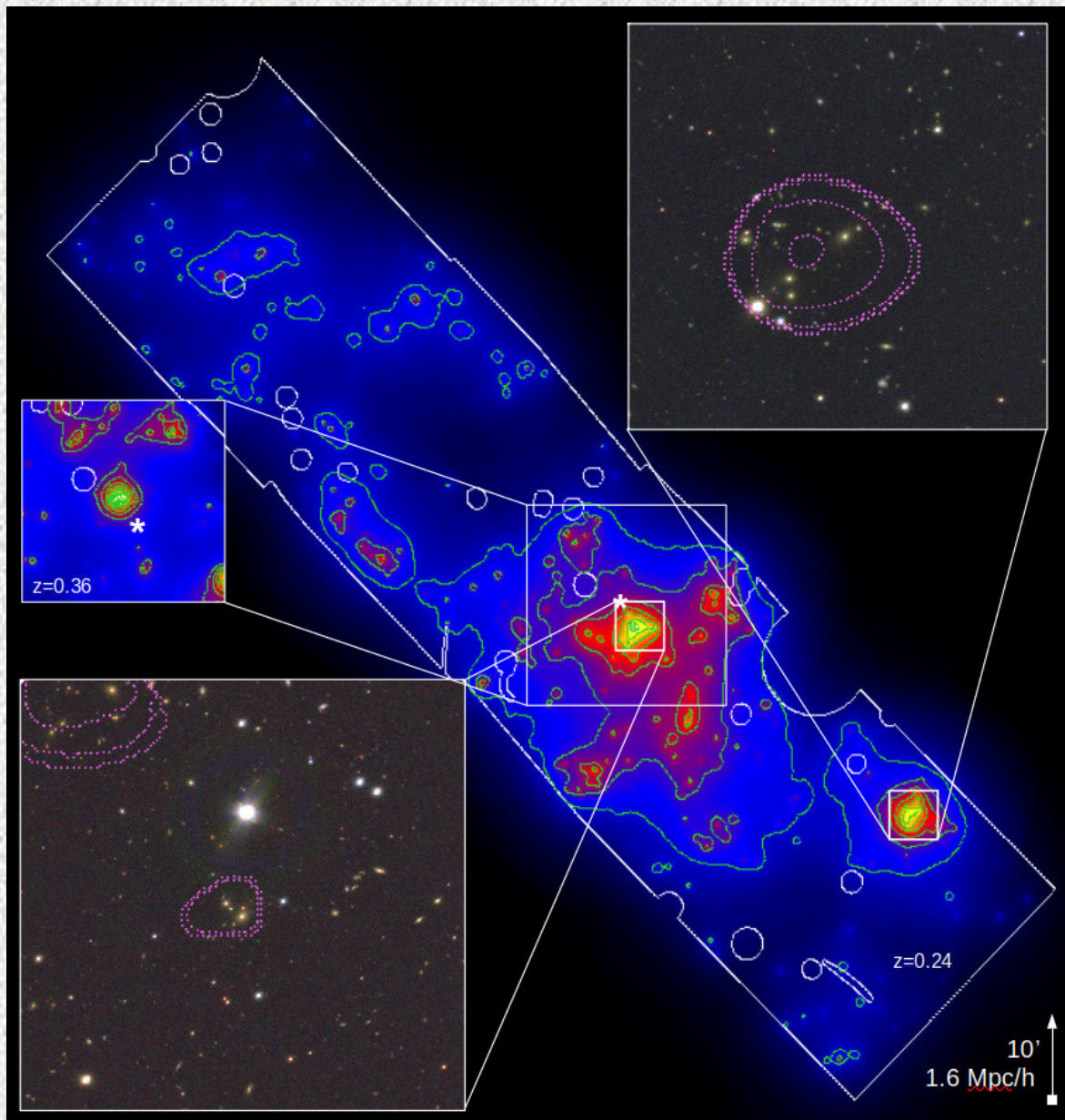
AMICO (Maturi+ 2023)
and
PzWav
(Doubrawa+2023)

Clusters in miniJPAS



Bonoli et al., 2021.

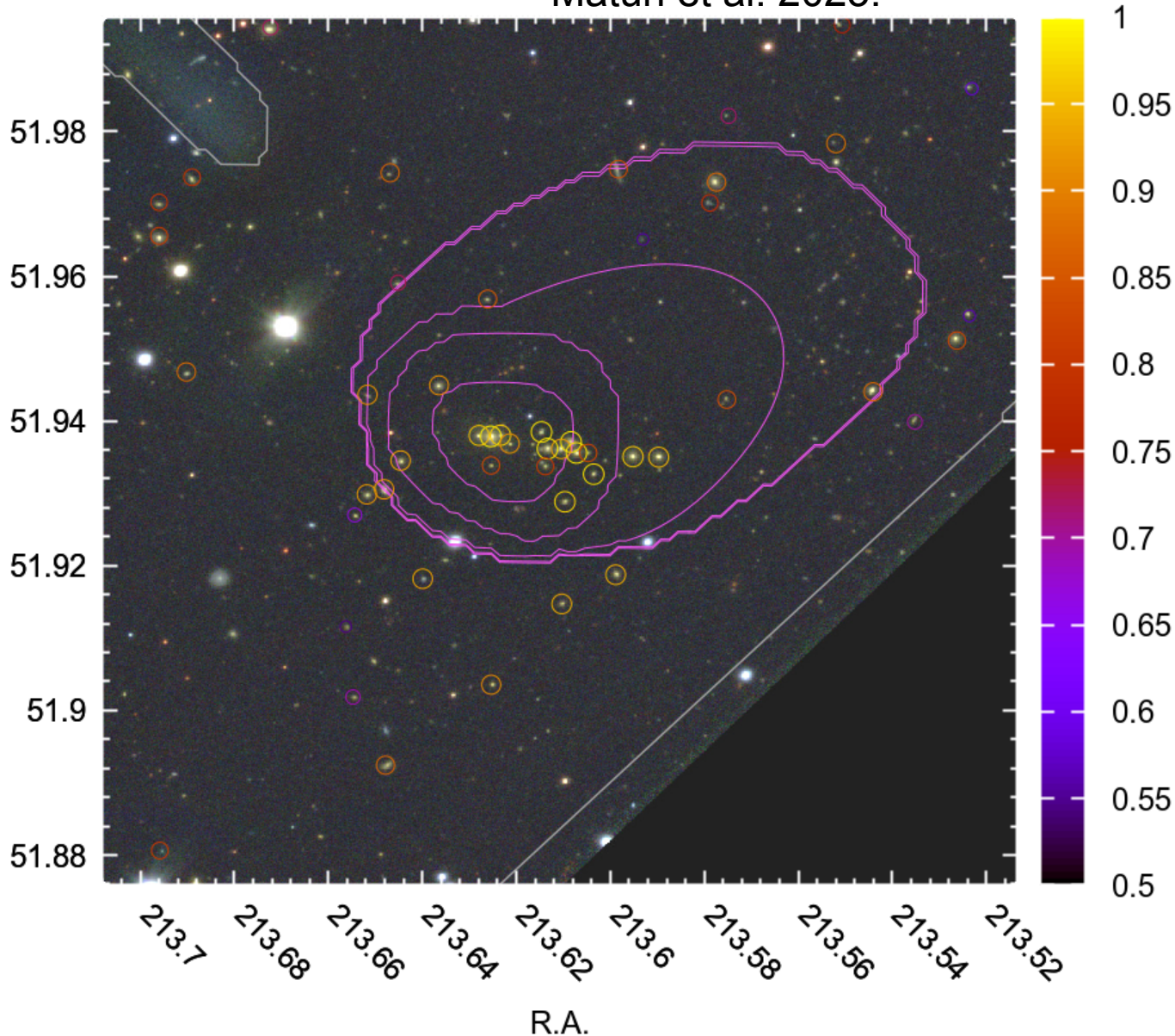
Fig. 27: The most massive cluster found in the miniJPAS footprint, centred at RA=213.6254, DEC=51.9379. This cluster is also part of the redMaPPer catalogue where it is listed as a cluster with richness $\lambda = 35$. The brightest galaxy has a spectroscopic redshift $z = 0.289$.



AMICO response to a redshift slice on $z \sim 0.24$, dashed iso-contours correspond to **X-ray data**

Maturi et al. 2023.

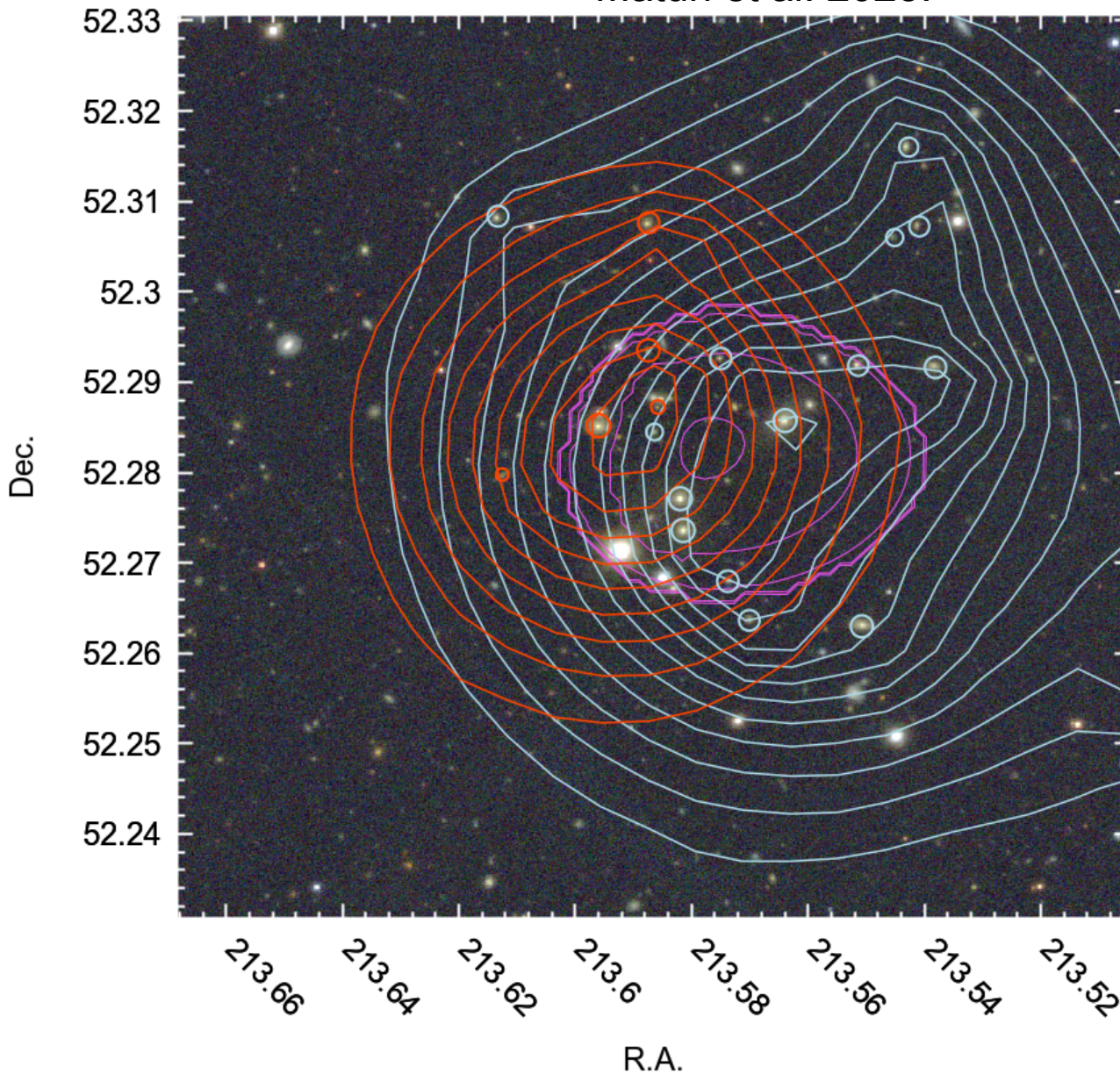
Maturi et al. 2023.



Contours are provided by **X-ray** data, color bar renders **membership probability** for each galaxy assigned by **AMICO**

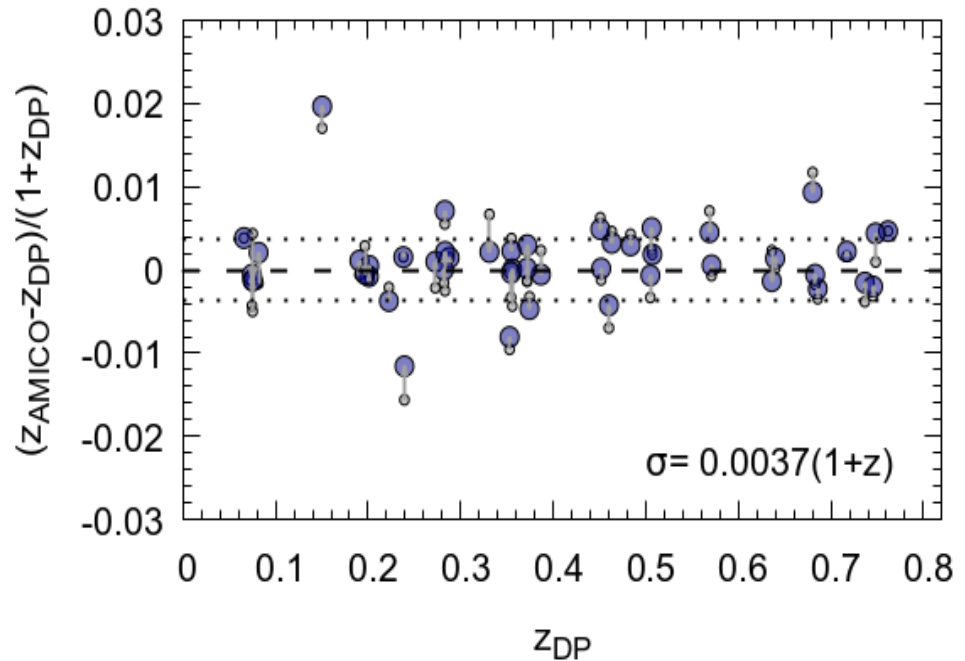
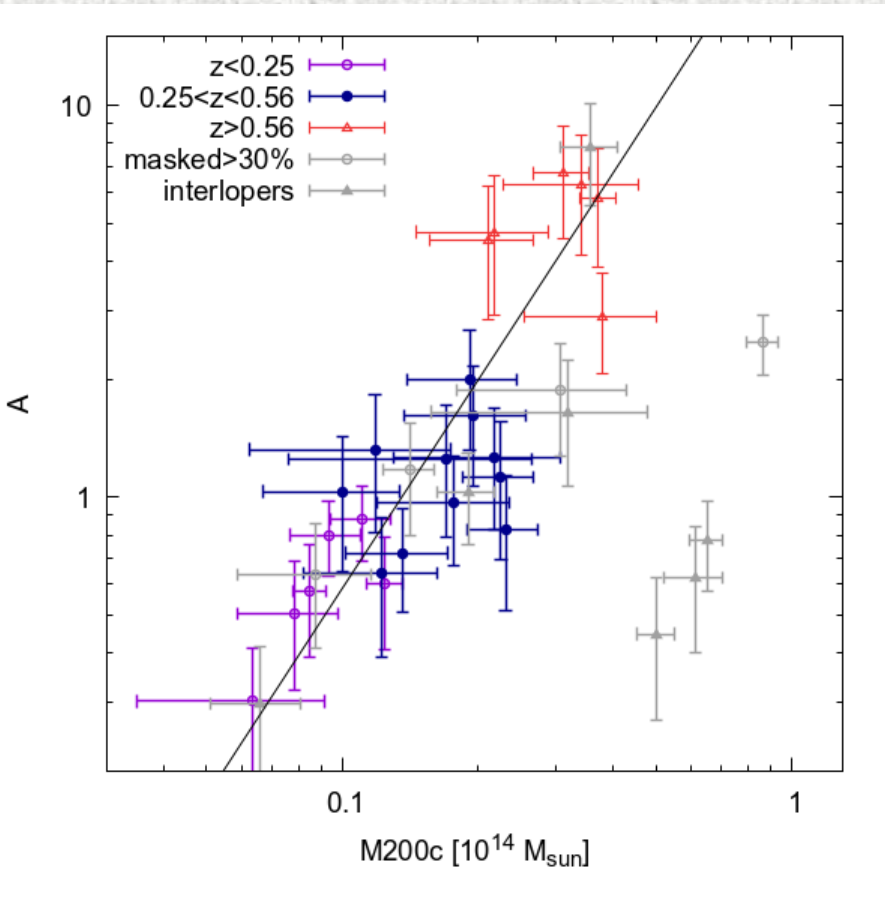
From **membership** we can assign total **luminosities** and **stellar masses** to clusters

Maturi et al. 2023.



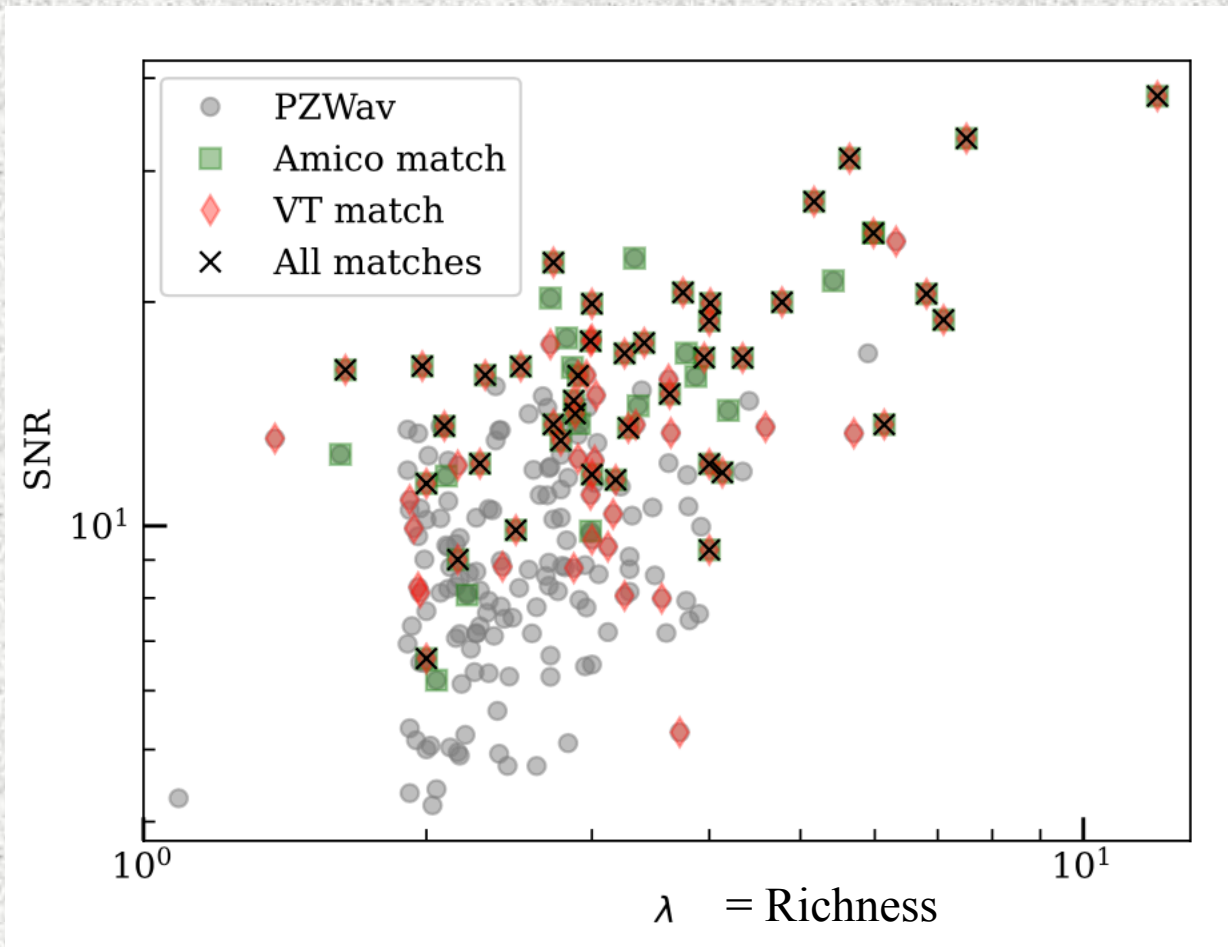
We can
distinguish
interloping
clusters/groups
along **very similar**
lines of sight...

Maturi et al. 2023.



Low scatter in mass proxy – mass relation for Individual clusters (no binning/stacking)

Very **accurate & precise** redshift determination for clusters:
We shall be able to conduct **galaxy cluster clustering**



Doubrawa+ 2023: Comparing **different group finders**:
Voronoi Tessellation (VT), AMICO, and PzWav.

Clusters in miniJPAS

- **~95 groups** with $M_{200} > 10^{13} M_{\odot}$ in **~1 sq.deg** with high levels of purity and completeness up to $z \sim 0.4$
- Internal weak lensing cluster mass estimates expected to give $\Delta \log M \sim 3\%$ or $\Delta \sigma_8 \sim 1.5\%$
- Current work towards establishing **density-based membership assignments** as a proxy for **optical mass**

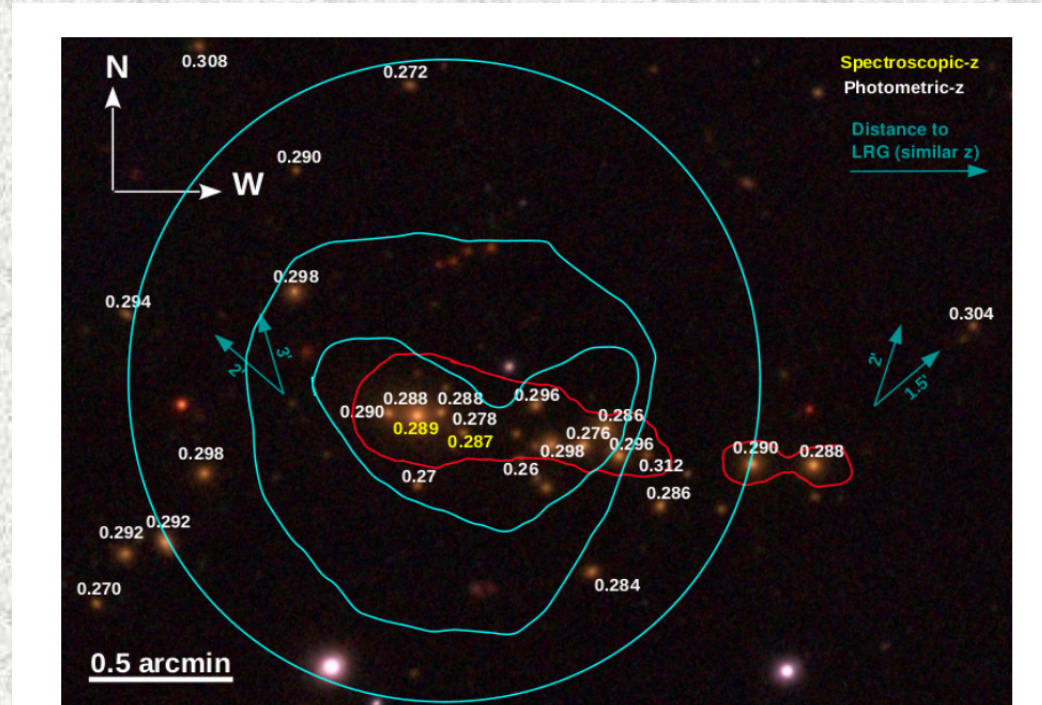
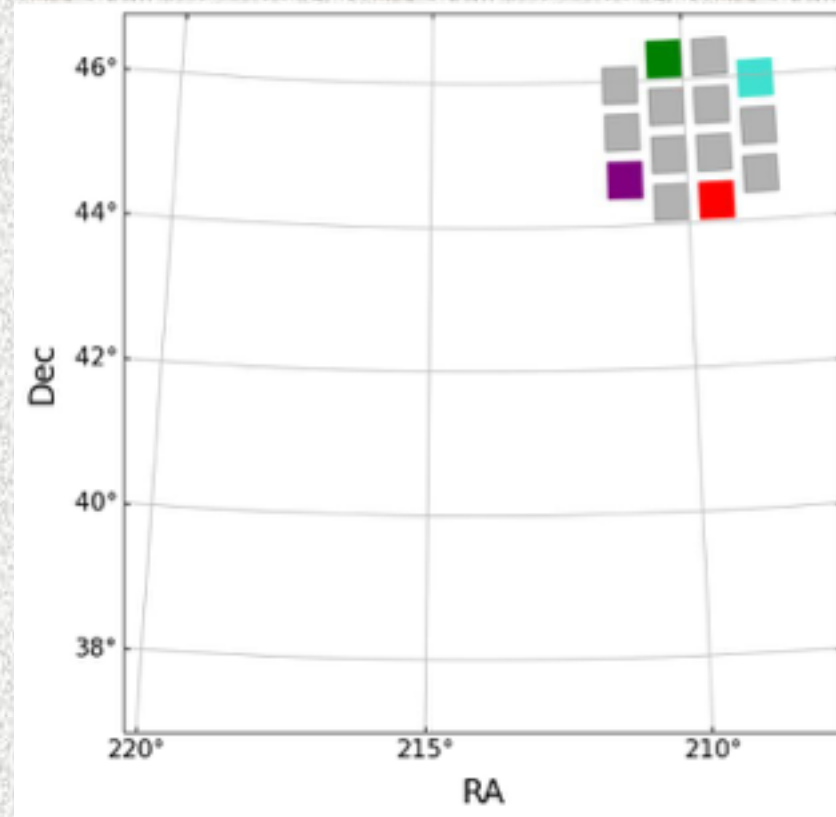


Fig. 27: The most massive cluster found in the miniJPAS footprint, centred at RA=213.6254, DEC=51.9379. This cluster is also part of the redMaPPer catalogue where it is listed as a cluster with richness $\lambda = 33$. The brightest galaxy has a spectro-

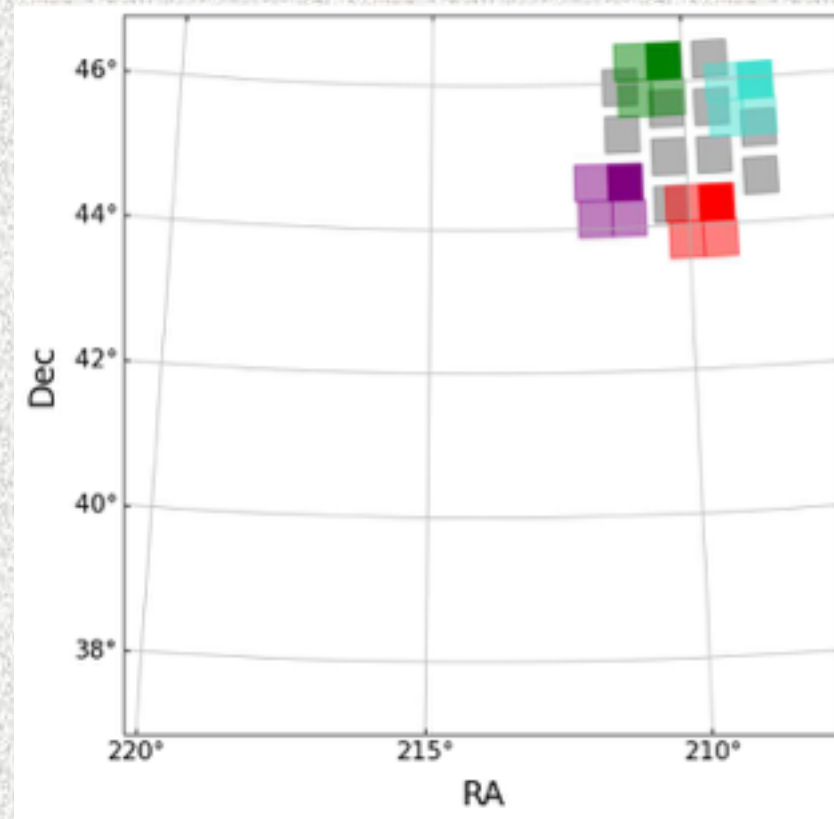
Bonoli et al. 2021

Current status and future prospects

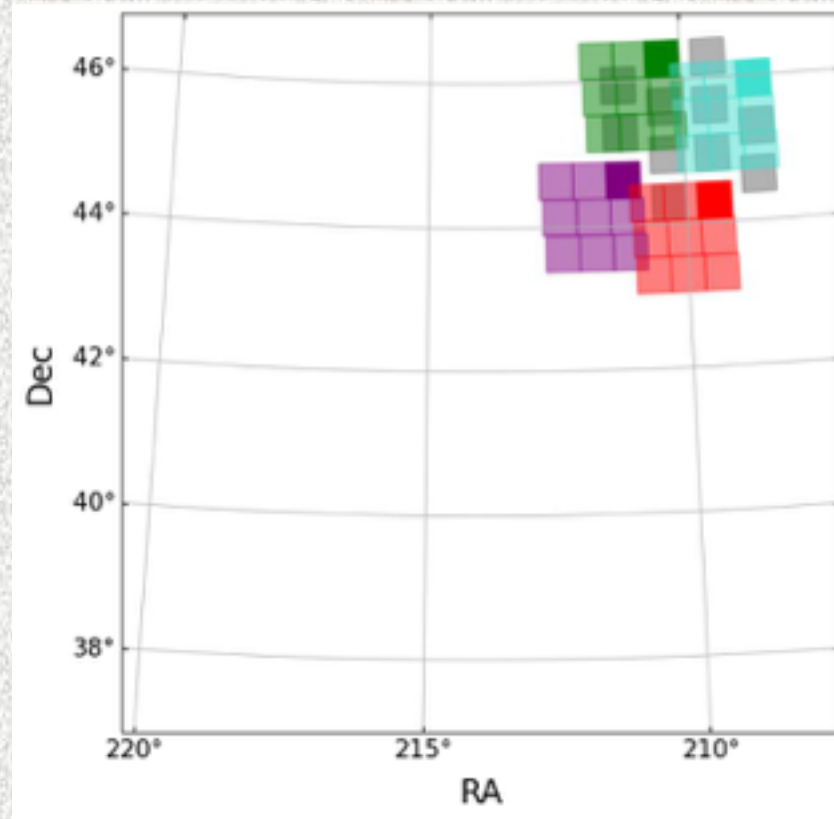
Growth of area covered in all filters



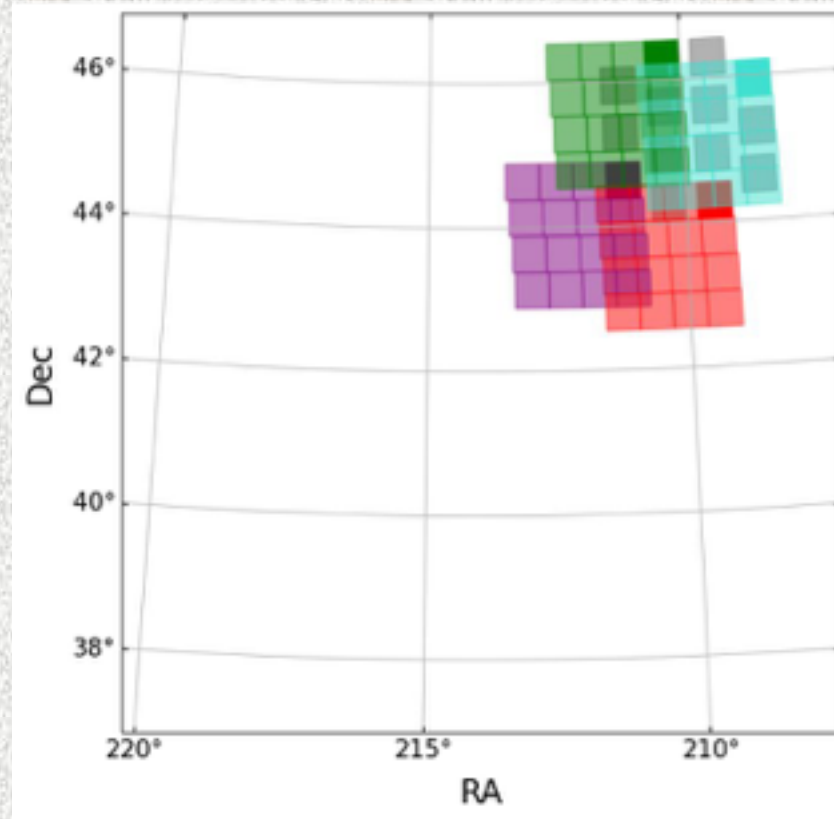
Growth of area covered in all filters



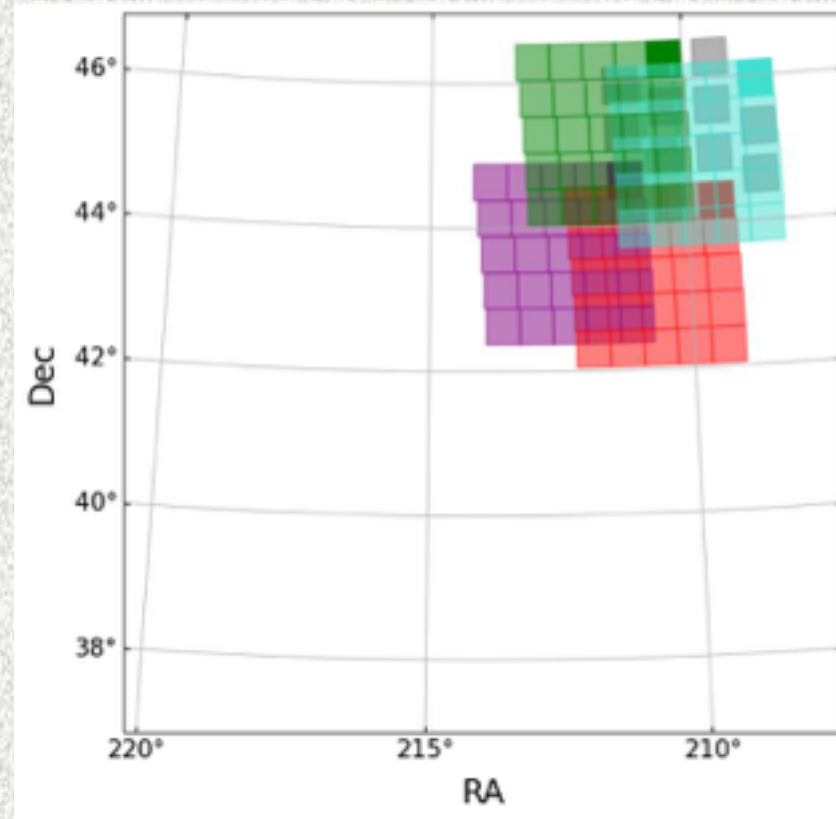
Growth of area covered in all filters



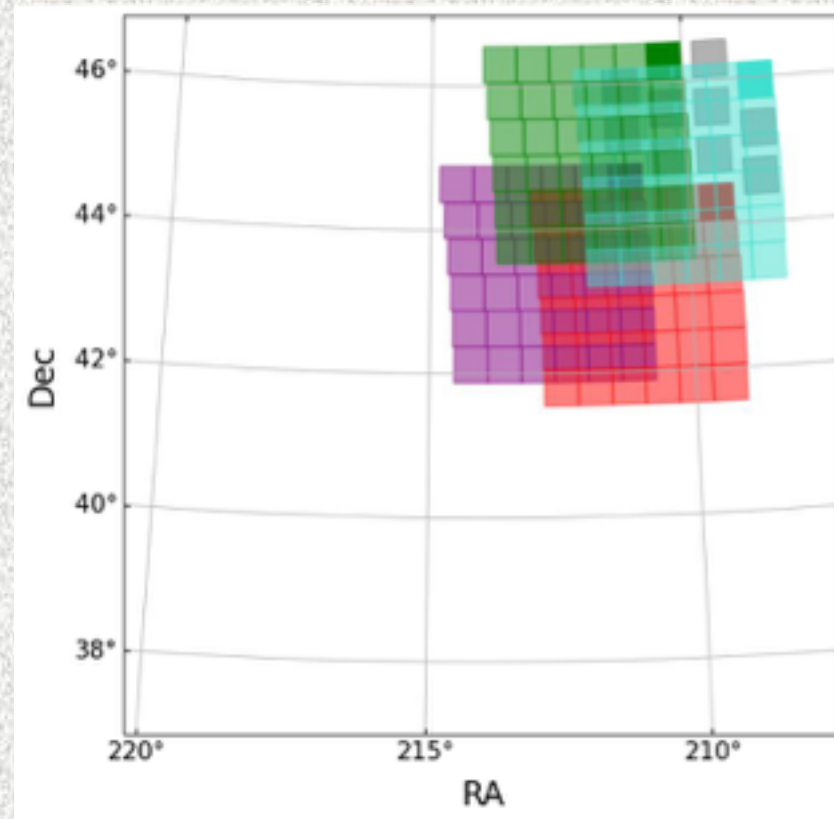
Growth of area covered in all filters



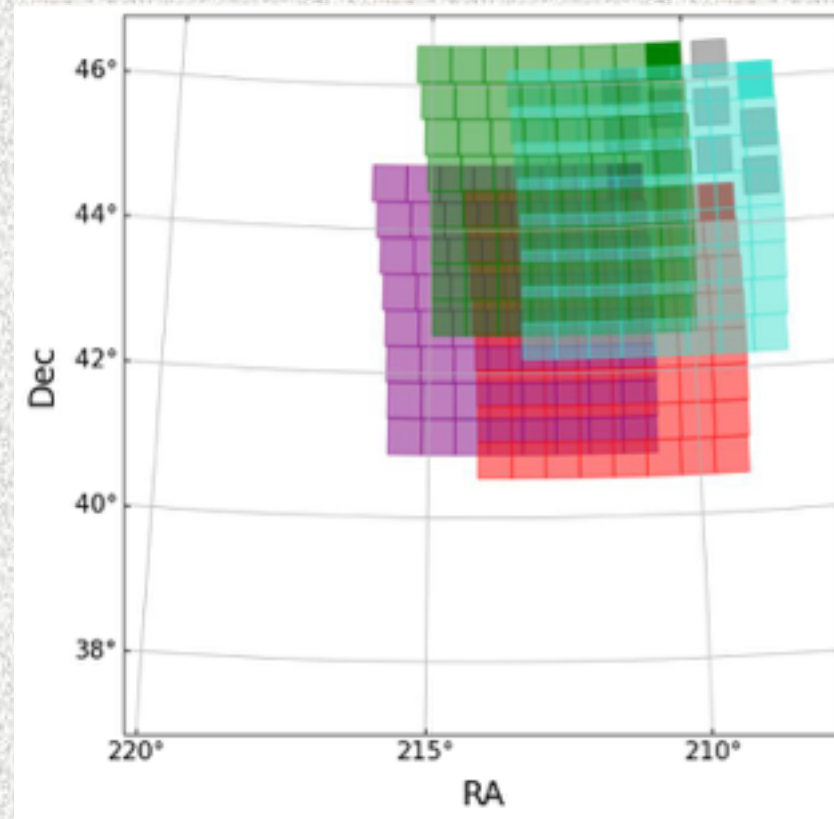
Growth of area covered in all filters



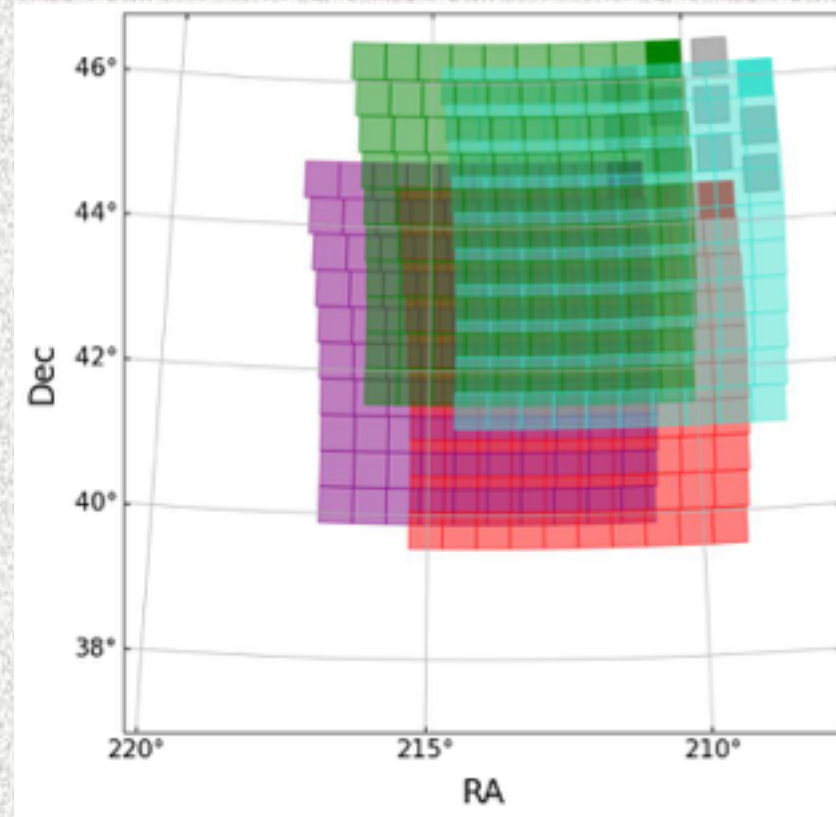
Growth of area covered in all filters



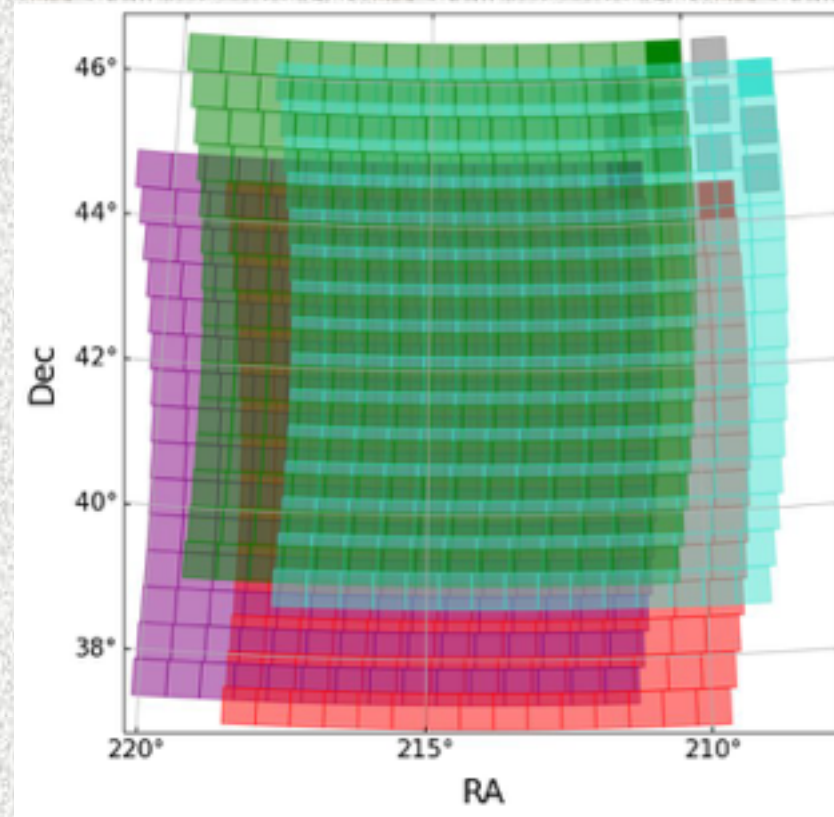
Growth of area covered in all filters



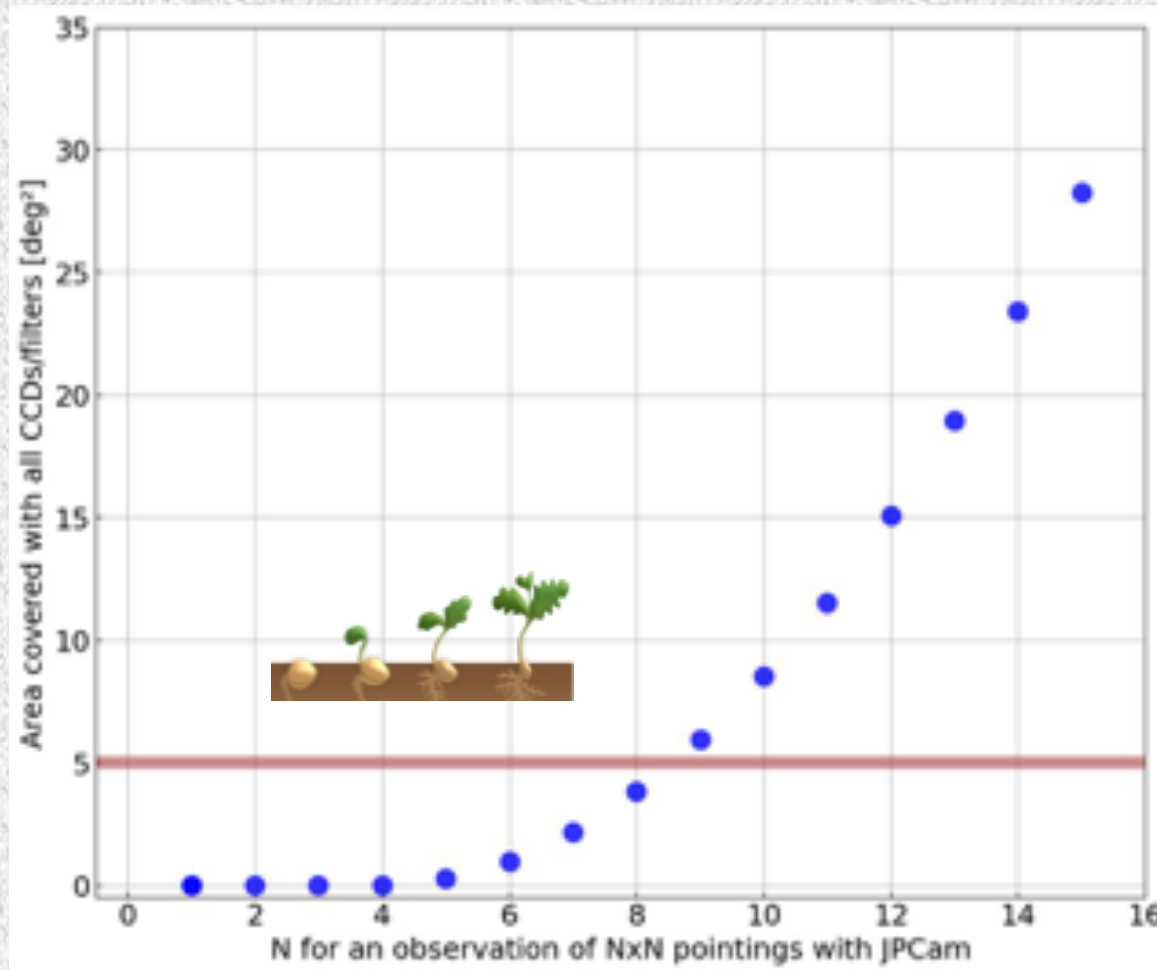
Growth of area covered in all filters



Growth of area covered in all filters

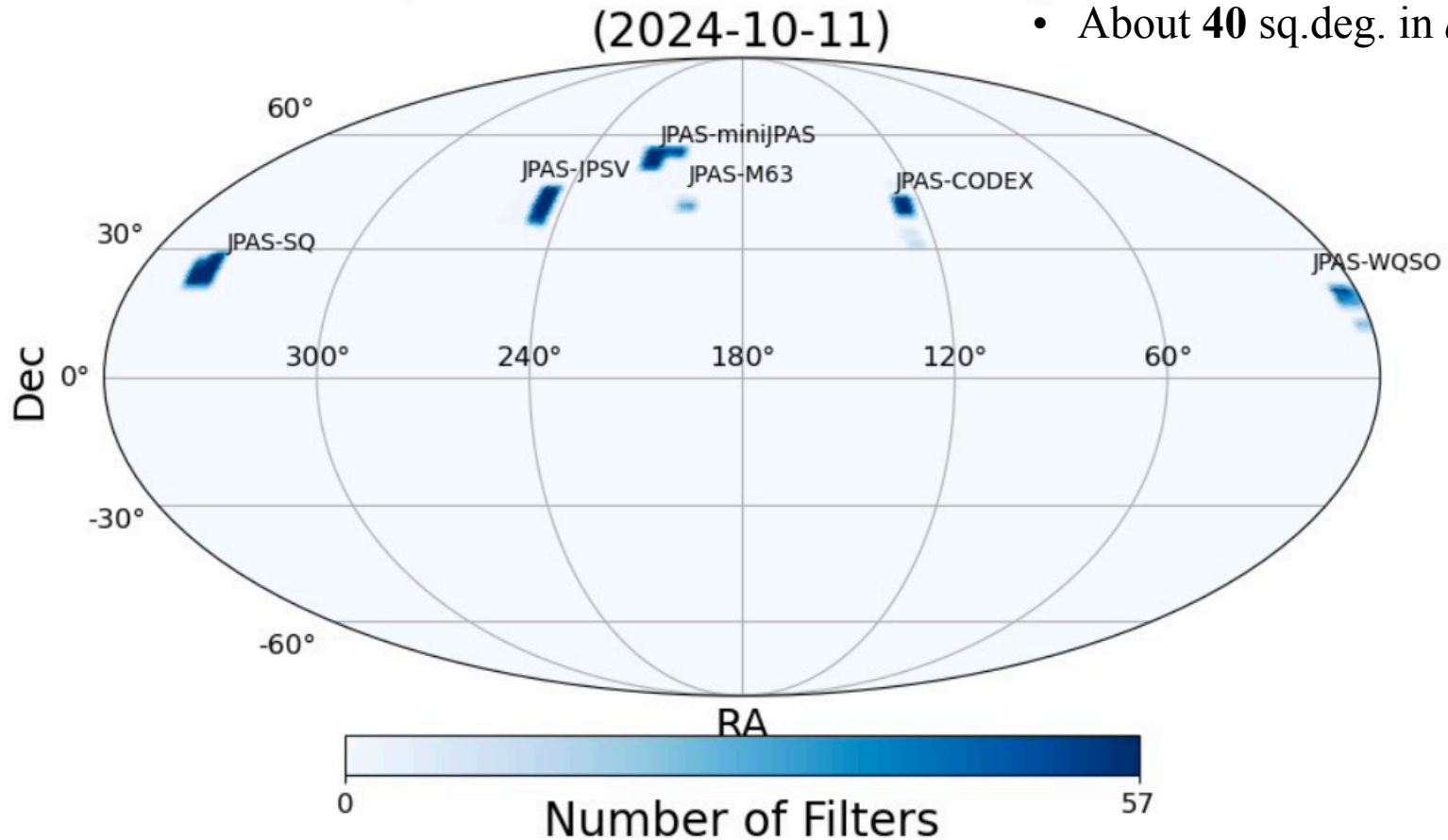


Growth of area covered in all filters

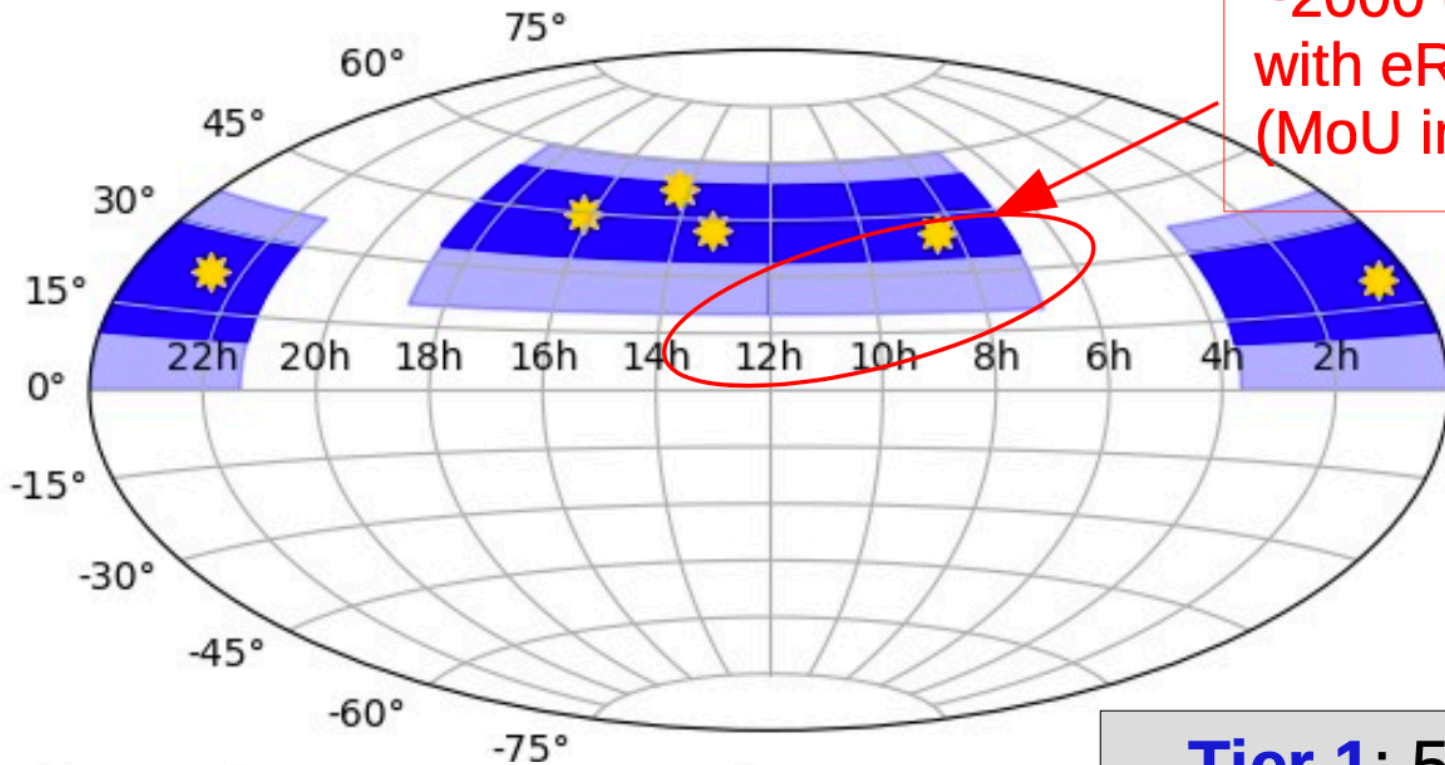


Current status

- About **500** sq.deg in *any* band
- About **40** sq.deg. in *all* bands

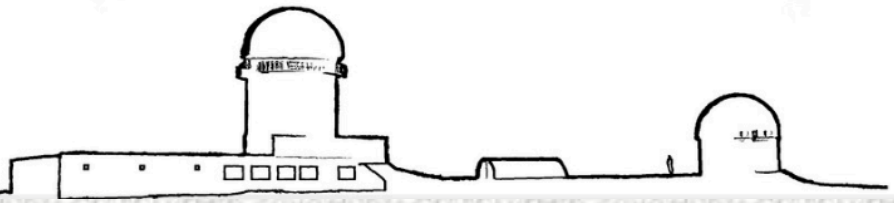


Survey growing around 6 *seeds*



~2000 deg² overlap
with eROSITA-DE
(MoU in place)

Tier 1: 5200 deg²
Tier 2: 8500 deg²



Take Home messages

- **54 NB + 3 MB/BB filters** over **~8,500 sq.deg**
- **4.5 deg² FoV**
- Up to mag~ **24.5 in BB filters**, **~ 22.5 in NB ones**
- 90M ELG and LRG
- Reaching **~0.3% photo-z precision for ~1/3rd of galaxies**
- Millions of QSOs at similar level of precision (**~0.3—0.5%**)
- 200M of galaxies
- **~700K of groups and clusters** with accurate photo-z and memberships
- **~10 sq.deg of J-PAS data** to be public in **November 2024**
- You can already access real miniJPAS & J-NEP data at <https://archive.cefca.es/catalogues>
- <http://www.j-pas.org>

<https://archive.cefca.es/catalogues>

The screenshot displays the Mini J-PAS web interface. At the top, the URL <https://archive.cefca.es/catalogues/minijpas-pdr201912/navigator.html> is shown in the browser's address bar. The interface includes a search bar with the text "Sky Navigator search" and input fields for "Object name:", "RA:" (14:17:47.628), and "DEC:" (52:41:43.74). A "Search" button is present. Below the search bar, a spectral plot for "Object: 2243 - 8101" is displayed. The plot shows Magnitude (y-axis, 16 to 26) versus Wavelength [Å] (x-axis, 3,000 to 10,000). The plot includes a legend for "MAG_AUTO" and "MAG", and a dropdown menu for "AUTO". A "RESET" button is located below the plot. To the right of the plot, a star field view is shown with a tooltip for "Object: 2243-8101" containing the following information: "Image Name: AEGIS002-v201912_rSDSS_swp", "RA, Dec (deg): 214.7034, 52.6958", "Class star: 0.0039", and "PhotoZ: 0.26". The tooltip also includes buttons for "Images" and "Explore Object". At the bottom of the interface, there is a copyright notice: "Copyright © 2018-2024 Javalambre Physics of the Accelerating Universe Astrophysical Survey. All Rights Reserved." and a footer: "Developed and maintained by Tamara Civera (CEFCA)".

Take Home messages

- **54 NB + 3 MB/BB filters** over **~8,500 sq.deg**
- **4.5 deg² FoV**
- Up to mag~ **24.5 in BB filters**, **~ 22.5 in NB ones**
- 90M ELG and LRG
- Reaching **~0.3% photo-z precision for ~1/3rd of galaxies**
- Millions of QSOs at similar level of precision (**~0.3—0.5%**)
- 200M of galaxies
- **~700K of groups and clusters** with accurate photo-z and memberships
- **~10 sq.deg of J-PAS data** to be public in **November 2024**
- You can already access real miniJPAS & J-NEP data at <https://archive.cefca.es/catalogues>
- <http://www.j-pas.org>

Take Home messages

- **54 NB + 3 MB/BB filters** over **~8,500 sq.deg**
- **4.5 deg² FoV**
- Up to mag~ **24.5 in BB filters**, **~ 22.5 in NB ones**
- **90M ELG and LRG**
- Reaching **~0.3% photo-z precision for ~1/3rd of galaxies**
- Millions of QSOs at similar level of precision (**~0.3—0.5%**)
- **200M of galaxies**
- **~700K of groups and clusters** with accurate photo-z and memberships
- **~10 sq.deg of J-PAS data** to be public in **November 2024**
- You can already access real miniJPAS & J-NEP data at <https://archive.cefca.es/catalogues>
- <http://www.j-pas.org>

